Molecular Phylogenetics and Evolution 91 (2015) 160–177

Contents lists available at ScienceDirect

Molecular Phylogenetics and Evolution

journal homepage: www.elsevier.com/locate/ympev

Oxytocin receptor gene sequences in owl monkeys and other primates show remarkable interspecific regulatory and protein coding variation ☆

Paul L. Babb [a,1], Eduardo Fernandez-Duque [a,b,c,*], Theodore G. Schurr [a,*]

[a] Department of Anthropology, University of Pennsylvania, Philadelphia, PA 19104, USA
[b] Centro de Ecología Aplicada del Litoral (CECOAL), Conicet, Corrientes, Argentina
[c] Facultad de Recursos Naturales, Universidad Nacional de Formosa, Formosa, Argentina

ARTICLE INFO

Article history:
Received 12 August 2014
Revised 11 April 2015
Accepted 8 May 2015
Available online 27 May 2015

Keywords:
OXTR
Behavioral genetics
Night monkey
Neurogenetics
Evolution

ABSTRACT

The oxytocin (OT) hormone pathway is involved in numerous physiological processes, and one of its receptor genes (*OXTR*) has been implicated in pair bonding behavior in mammalian lineages. This observation is important for understanding social monogamy in primates, which occurs in only a small subset of taxa, including Azara's owl monkey (*Aotus azarae*). To examine the potential relationship between social monogamy and *OXTR* variation, we sequenced its 5′ regulatory (4936 bp) and coding (1167 bp) regions in 25 owl monkeys from the Argentinean Gran Chaco, and examined *OXTR* sequences from 1092 humans from the 1000 Genomes Project. We also assessed interspecific variation of *OXTR* in 25 primate and rodent species that represent a set of phylogenetically and behaviorally disparate taxa. Our analysis revealed substantial variation in the putative 5′ regulatory region of *OXTR*, with marked structural differences across primate taxa, particularly for humans and chimpanzees, which exhibited unique patterns of large motifs of dinucleotide A + T repeats upstream of the *OXTR* 5′ UTR. In addition, we observed a large number of amino acid substitutions in the *OXTR* CDS region among New World primate taxa that distinguish them from Old World primates. Furthermore, primate taxa traditionally defined as socially monogamous (e.g., gibbons, owl monkeys, titi monkeys, and saki monkeys) all exhibited different amino acid motifs for their respective *OXTR* protein coding sequences. These findings support the notion that monogamy has evolved independently in Old World and New World primates, and that it has done so through different molecular mechanisms, not exclusively through the oxytocin pathway.

1. Introduction

Monogamous social systems are rarely observed among primates, yet are widely distributed geographically and phylogenetically across the order. This pattern indicates that social monogamy has arisen independently multiple times throughout primate evolution (Fuentes, 1999; Brotherton and Komers, 2003; Lukas and Clutton-Brock, 2013). Although "social monogamy" necessarily involves many different complex social behaviors (Mendoza et al., 2002; Moller, 2003; Huck et al., 2014), its occurrence raises the important question of whether some of the social behaviors of different primate taxa are controlled by the same genes. In other words, can the observed differences at specific genetic loci explain the spectrum and distribution of social behaviors in primates?

There is growing evidence that certain molecular pathways and neurogenetic loci play key roles in the expression of social behavior in mammals. Of these, the pathway involving the neuropeptide hormone oxytocin (OT, 9 amino acids) and its neuron-based oxytocin receptor protein (OXTR or OT-R, 389 amino acids) has been linked to mammalian social behaviors and emotional states that promote sociality (Carter, 1998; Carter et al., 2008; Skuse et al., 2014; Wittig et al., 2014). Synthesized in the hypothalamus, OT is a multifunctional peptide that signals to *OXTR* G-protein coupled receptors via osmotic cellular diffusion across cell membranes (reviewed in Carter et al., 2008).

As a signal transmitter, OT coordinates social behaviors within the neuroendocrine network, where it responds to the activity of various stressors by reducing reactivity or promoting withdrawal

☆ This paper was edited by the Associate Editor Derek Wildman.

* Corresponding authors at: Department of Anthropology, Yale University, 10 Sachem Street, Room 314, New Haven, CT 06511, USA (E. Fernandez-Duque). Department of Anthropology, University of Pennsylvania, 432 University Museum, 3260 South Street, Philadelphia, PA 19104-6398, USA. Fax: +1 215 898 7462 (T.G. Schurr).

E-mail addresses: eduardo.fernandez-duque@yale.edu (E. Fernandez-Duque), tgschurr@sas.upenn.edu (T.G. Schurr).

[1] Present address: Department of Pharmacology, Perelman School of Medicine at the University of Pennsylvania, Philadelphia, PA 19104, USA.

http://dx.doi.org/10.1016/j.ympev.2015.05.006
1055-7903/

(Grippo et al., 2008, 2009). OT interacts with neural pathways involved in processing motivationally relevant stimuli through its influence on the mesocorticolimbic dopamine system (Damiano et al., 2014). Functioning in these ways, OT plays an important role in positive social interactions, such as grooming, sex, childbirth and parental care (Carter et al., 2008). OT has also been associated with social signaling (Bales et al., 2007a; Bales et al., 2007b; Bales et al., 2007c), and deficits in the processing of social information have been linked to low OT levels (Takayanagi et al., 2005).

Furthermore, it has been suggested that the social deficits in certain autism spectrum disorders in humans might be related to low levels of OT (Wu et al., 2005; Jacob et al., 2007; Gregory et al., 2009), although inconsistent findings relating oxytocin to autism have been noted (Tansey et al., 2010). On the other hand, human generosity has been tied to the OT pathway (Barraza and Zak, 2009), and common genetic polymorphisms in *OXTR* are associated with stress reduction (Chen et al., 2011), empathy (Wu et al., 2012), face recognition memory skills (Skuse et al., 2014) and human hypothalamic limbic structure and function (Tost et al., 2010). Hence, there is abundant evidence showing that the neuroendocrine OT pathway is integral to developing and maintaining social relationships between individuals.

As such, OT has been implicated in long-term affiliative behaviors that are associated with social interactions, such as huddling, aggression reduction, mating and the formation of temporally pervasive social bonds. Research on knockout mice has shown that the pair bonding and offspring investment behaviors that typify affiliative social interactions between individual mice are not manifested when the actions of OT are blocked (Takayanagi et al., 2005). Similarly, studies have implicated OT in the manifestation of pro-social and pair bonding behaviors in primates (Bales et al., 2007a; Snowdon et al., 2010; Smith et al., 2010; Cavanaugh et al., 2014).

Yet, the mechanics underlying the OT pathway are clearly different in primates than in rodents. A novel form of OT (Leu8Pro) was shown to exist in taxa belonging to the family Cebidae (*Cebus*, *Saimiri*, *Aotus*, and *Callithrix* spp., *sensu* Perelman et al., 2011) of New World primates (parvorder Platyrrhini; denoted as NWP) that distinguishes them from all other primates, including Old World primates (parvorder Catarrhini; denoted as OWP) and hominoid apes (superfamily Hominoidea; denoted as APES), suggesting that the OT system does not function identically across all primate taxa (Lee et al., 2011). More recently, researchers uncovered three additional isoforms of OT in NWP, and noted that several non-synonymous amino acid changes in the *OXTR* gene were present in those primate taxa, suggesting that the OT ligand and OXTR receptor molecules likely co-evolved in primates (Vargas-Pinilla et al., 2015). Given these findings, and considering the broad range of social behaviors exhibited by primates, one can envision that lineage-specific mutations at the *OXTR* locus may have induced functional changes to the OT pathway, and ultimately influenced the differential evolution of sociality in different lineages of primates. However, little is known about the extent of sequence variation that exists at the regulatory promoter region upstream of *OXTR* in different primate lineages, and the degree to which regulatory or coding variation in the primate *OXTR* gene correlates with primate social systems remains unclear.

Despite their overall rarity, monogamous social systems are particularly enriched among the NWP (Fuentes, 1999; Lukas and Clutton-Brock, 2013). Azara's owl monkeys (*Aotus azarae*) from Formosa, Argentina, exhibit many of the behaviors associated with monogamous social systems (Fernandez-Duque, 2009). These behaviors include a long enduring pair bond between adults, biparental care of infants, territoriality, and food sharing (Wolovich et al., 2008; Huck and Fernandez-Duque, 2013; Wartmann et al., 2014; Fernandez-Duque, 2015). Furthermore, recent evidence shows that wild Azara's owl monkeys are also genetically monogamous, as well (Huck et al., 2014).

These behavioral attributes make *A. azarae* an ideal model in which to investigate the potential role of genetics in influencing social and mating behavior. To that end, through our analyses of Azara's owl monkeys *OXTR* variation and social behavior, we tested the following predictions: (1) few *OXTR* regulatory and coding mutations will segregate within primate populations; (2) many *OXTR* mutations will distinguish different phylogenetic lineages of primates; (3) *OXTR* coding mutations will be enriched in functional protein domains; and (4) *OXTR* mutations will cluster with primate taxa that exhibit similar forms of complex social behaviors, with one specific proxy being population-level monogamous social systems.

To evaluate these predictions, we investigated *OXTR* sequence diversity in primates at multiple levels. First, to assess intraspecific variation at the *OXTR* locus, we sequenced 4936 base pairs (bp) of the putative 5′ regulatory region and the entire 1167 bp coding region (CDS) in a wild *A. azarae* population, and analyzed orthologous regions in a larger *Homo sapiens* data set from the 1000 Genomes Project (1000 Genomes Project Consortium, 2010, 2012). Next, to investigate interspecific variation at the *OXTR* locus, we analyzed ~5 kb of putative 5′ regulatory region from eight primate genomes to identify potential mutations that could influence *OXTR* expression. We also examined the *OXTR* CDS from 37 primates and two rodents to identify all amino acid substitutions and reconstruct the molecular history of the *OXTR* locus among primates. Following this step, we partitioned the CDS into major *OXTR* functional protein domains (ligand-binding, G-protein binding, and transmembrane) to determine whether any of them were enriched for amino acid substitutions in primate populations or clades. Finally, we compared the patterns of observed *OXTR* 5′ regulatory mutations and domain-specific amino acid substitutions within particular primate phylogenetic clades and populations in order to identify evidence for the clustering of *OXTR* mutations with specific forms of primate social systems, and to determine whether they can explain the differential evolution of sociality in different lineages of primates.

2. Methods

2.1. Study population

The wild *A. azarae* study population inhabits gallery forests and the forest-islands along the Rio Pilagá located in the northern province of Formosa, Argentina, in the South American Gran Chaco. Owl monkeys are socially and genetically monogamous, and social groups are generally comprised of 2–6 individuals, with only a single pair of reproductive adults (Fernandez-Duque et al., 2001; Fernandez-Duque and Huck, 2013). Male owl monkeys typically become the primary carriers of their offspring one week after birth, and in general infants only return to the mothers to nurse (Rotundo et al., 2005; Wolovich et al., 2008; Huck and Fernandez-Duque, 2013). This pattern of social and genetic monogamy and intensive paternal care distinguishes owl monkeys from the majority of other primate taxa.

2.2. Samples

To assess intraspecific variation of *OXTR* in Azara's owl monkeys we isolated DNA from 25 *A. azarae* individuals using tissue, blood, feces, hair, and placental samples (Babb et al. 2010, 2011a, 2011b). This panel included twenty-one residents of the study site population, and four captive individuals from the Saenz-Peña Municipal Zoo (Saenz-Peña, Chaco Province, Argentina). These owl monkey

samples represent diverse mitochondrial lineages in the study population (Babb et al. 2011a), and do not include related individuals (Huck et al., 2014) (Table 1).

To examine intraspecific variation of *OXTR* in humans, we accessed the most recent release of the 1000 Genomes Project (1KG) Phase 1 genotype data set (index 20101123). This data set features 1092 individuals from 14 populations with recorded variation at more than 37 million genetic loci (1000 Genomes Project Consortium, 2010, 2012) (Table 1). We downloaded the .vcf file for chromosome 3 from NCBI (ftp://ftp-trace.ncbi.nih.gov/1000genomes/ftp/), and filtered the data to include only 1759 single nucleotide polymorphism (SNP) genotypes for 1092 individuals in an 115,211 bp window spanning from 50 kilobases (kb) upstream of the *OXTR* gene start codon to 50 kb downstream of the *OXTR* gene stop codon (NM_000916, genome build hg19, chr3: 8,744,663–8,859,873). We further organized variants to reflect comparative regions of interest (SNPs in ~5 kb of the 5′-flanking non-coding putative regulatory region, and in 1167 bp of the CDS, which includes the ligand binding, G-protein binding, and transmembrane domains), and performed text manipulation of 1KG VCFs using Perl and VCFtools v0.1.12 (Danecek et al., 2011).

For interspecific analyses of *OXTR*, we obtained DNA samples from three *Aotus* species and subspecies (*A. nancymaae*, *A. lemurinus*, and *A. nigriceps*), two titi monkey individuals (*Callicebus donacophilus*), two saki monkey individuals (*Pithecia pithecia*), and two squirrel monkey individuals (*Saimiri sciureus*) from the Zoological Society of San Diego (ZSSD) (San Diego, CA). We acquired five *A. nancymaae* DNA samples from individuals living at the DuMond Conservancy for Primates and Tropical Forests (Miami, FL). In addition, we acquired DNA samples for 13 primate taxa from the NIA and IPBIR cell line collections curated by the Coriell Institute of Biomedical Research (Camden, NJ), and one commercially available human DNA sample (Promega control human DNA [G304A]) (Table 1). Lastly, we conducted searches of GenBank (NCBI), the University of California-Santa Cruz Genome Browser (UCSC GB) and the European Bioinformatics Institute's ENSEMBL browser for genomic sequence surrounding the *OXTR* locus in primates and rodents, and obtained *OXTR* regulatory and coding sequences for eight primate species and two rodent species (Kent, 2002; Kent et al., 2002; Flicek et al., 2011) (Table 1). In total, we analyzed 25 *A. azarae* and 1092 *H. sapiens* individuals for intraspecific analyses, whereas our interspecific analyses focused on 39 individuals (inclusive of AAPLunk) representing 25 species and subspecies, including 12 NWP taxa, four OWP taxa, seven APE taxa, and two rodent taxa as phylogenetic outgroups.

2.3. DNA sequencing

To assess variation in *OXTR*, we targeted the coding region (1167 bp, 2 amino acid-coding exons) and the adjacent 5′-flanking non-coding putative regulatory region (~5000 bp) (Kimura et al., 1992; Inoue et al., 1994; Gimpl and Fahrenholz, 2001). We identified *OXTR* sequencing targets by assembling multisequence alignments of genomic sequence files from UCSC GB using Geneious Pro v5.6.7 (Drummond et al., 2010) (Fig. 1). From this assembly, we identified regions exhibiting high levels of sequence conservation across all taxa and designed primers with NetPrimer (Premier BioSoft) and Primer3 to align to them (Rozen and Skaletsky, 2000) (Table 2). We used the primers to generate 10 overlapping amplicons (~700 bp each) for the 5′-flanking regulatory region and the first amino acid-coding exon (exon 3), and produced a single amplicon for exon 4. We optimized PCR cycling parameters using a Touchgene Gradient thermocycler (Techne), and amplified subsequent reactions using GeneAmp 9700 thermocyclers (ABI). We purified PCR amplicons through SAP/Exo I digestion (NEB), and sequenced all fragments on a 3130*xl* Gene Analyzer (ABI). We assessed read quality for each sequence using Sequencing Analysis v5.4 (ABI). We created individual contigs for each sample by aligning overlapping forward and reverse reads for each amplicon (95% agreement threshold), and tiled the consecutive amplicon contigs using Geneious Pro. Following this approach, we assembled 4936 bp of *OXTR* 5′ regulatory sequence and 1167 bp of CDS sequence for each *A. azarae* individual, and complete *OXTR* CDS sequences for all other taxa.

2.4. Population genetic analyses

2.4.1. Intraspecific multisequence alignments

We organized *OXTR* 5′-flanking regulatory region and *OXTR* CDS region multisequence alignments (MSA) for both the *A. azarae* ($n = 25$) and the *H. sapiens* ($n = 1092$) sample sets, using the original multi-taxa genomic sequence alignment consensus as a guide. After gap removal, the *A. azarae* MSA for the *OXTR* 5′-flanking regulatory region was 4936 bp. Although not exclusively "regulatory" in nature, this region included many features important to the expression and regulation of *OXTR*, such as the entire 1.5 kb of the 5′ untranslated region (UTR), the two non-coding exons (exons 1 and 2), 3.4 kb of 5′ flanking sequence upstream of the transcriptional start site (TSS) which contained TATA-like and GATA-1 motifs, transcription factor binding sites, estrogen response elements (EREs) nucleofactor interleukin-6 (NF IL-6) binding sequences, and acute phase reactant responsive elements (Kimura et al., 1992; Inoue et al., 1994; Gimpl and Fahrenholz, 2001). For the *A. azarae* *OXTR* CDS MSA, we merged the sequences of the two amino acid-coding exons (exons 3 and 4), and trimmed the terminal stop codon (TGA), which resulted in a CDS MSA length of 1167 bp.

Similarly, we created *H. sapiens* MSAs by extracting orthologous regions of the 1KG reference genome (build: g1k_v37.fasta, 1000 Genomes Project Consortium, 2010, 2012), and then mapping the variants from the VCF file (minus strand, SNP positions from chr3: 8809944–8809162, and 8794870–8794707) to the reference in order to produce appropriate *OXTR* 5′ regulatory and CDS sequences for each sample. We subsequently aligned these individual sequences into a 5325 bp *H. sapiens* population *OXTR* 5′ regulatory region MSA, and a 1167 bp *H. sapiens* population *OXTR* CDS region MSA.

2.4.2. Intraspecific summary statistics

We generated summary statistics for both *A. azarae* and *H. sapiens* population data sets from their respective 5′ regulatory region and CDS MSAs using Geneious Pro and R (R Core Team, 2012, pegas package: Paradis, 2010, ape package: Paradis et al., 2004). For each population's MSAs, we investigated all polymorphic sites and calculated their respective minor allele frequencies (MAF) for the individual loci. To estimate overall alignment variation levels, we measured pairwise identity and nucleotide diversity (π) for each MSA (Nei and Li, 1979). We recorded GC content, transitions (TI), transversions (TV), and insertion/deletions for all alignments, and noted any putative amino acid substitutions for the CDS and protein domain MSAs. To explore potential demographic or selective evolutionary pressures that may have influenced the observed changes in our population-based intraspecific comparisons, we calculated Tajima's *D* (Tajima, 1989a, 1989b) using R:pegas.

2.5. Phylogenetic analyses

2.5.1. Interspecific multisequence alignments

For phylogenetic analyses of *OXTR* 5′ regulatory and coding sequences, we restricted the number of *A. azarae* sequences used in the analyses to one individual (AAPLunk) which possessed the

Table 1
Samples investigated at the *OXTR* locus.

Clade	ID	Species	Common Name	Mating System[a]	Sex	Source / Accession / Build
Aotus azarae	AAPLunk[b]	*Aotus azarae*	Azara's owl monkey	M	unk	core area, Formosa[c]
	AA008	*Aotus azarae*	Azara's owl monkey	M	m	core area, Formosa[c]
	AA014	*Aotus azarae*	Azara's owl monkey	M	m	core area, Formosa[c]
	AA015	*Aotus azarae*	Azara's owl monkey	M	f	core area, Formosa[c]
	AA021	*Aotus azarae*	Azara's owl monkey	M	m	core area, Formosa[c]
	AA032	*Aotus azarae*	Azara's owl monkey	M	f	core area, Formosa[c]
	AA034	*Aotus azarae*	Azara's owl monkey	M	f	core area, Formosa[c]
	AA037	*Aotus azarae*	Azara's owl monkey	M	f	core area, Formosa[c]
	AA053	*Aotus azarae*	Azara's owl monkey	M	m	core area, Formosa[c]
	AA057	*Aotus azarae*	Azara's owl monkey	M	m	core area, Formosa[c]
	AA063	*Aotus azarae*	Azara's owl monkey	M	m	core area, Formosa[c]
	AA067	*Aotus azarae*	Azara's owl monkey	M	f	core area, Formosa[c]
	AA071	*Aotus azarae*	Azara's owl monkey	M	m	downstream, Formosa[c]
	AA082	*Aotus azarae*	Azara's owl monkey	M	m	downstream, Formosa[c]
	AA087	*Aotus azarae*	Azara's owl monkey	M	f	core area, Formosa[c]
	AA092	*Aotus azarae*	Azara's owl monkey	M	m	core area, Formosa[c]
	AA108	*Aotus azarae*	Azara's owl monkey	M	f	upstream, Formosa[c]
	AA109	*Aotus azarae*	Azara's owl monkey	M	m	core area, Formosa[c]
	AA114	*Aotus azarae*	Azara's owl monkey	M	f	core area, Formosa[c]
	AA122	*Aotus azarae*	Azara's owl monkey	M	f	core area, Formosa[c]
	AA123	*Aotus azarae*	Azara's owl monkey	M	m	core area, Formosa[c]
	AAF1	*Aotus azarae*	Azara's owl monkey	M	f	Saenz-Peña Zoo[d]
	AAF1B	*Aotus azarae*	Azara's owl monkey	M	f	Saenz-Peña Zoo[d]
	AAF2	*Aotus azarae*	Azara's owl monkey	M	f	Saenz-Peña Zoo[d]
	AAM2	*Aotus azarae*	Azara's owl monkey	M	m	Saenz-Peña Zoo[d]
	AL01	*Aotus lemurinus*	lemurine owl monkey	M	m	San Diego Zoo / CRES[e]
	ANI01	*Aotus nigriceps*	black-headed owl monkey	M	m	San Diego Zoo / CRES[e]
	ANA01	*Aotus nancymaae*	Nancy Ma's owl monkey	M	f	San Diego Zoo / CRES[e]
	ANA02	*Aotus nancymaae*	Nancy Ma's owl monkey	M	f	DuMond Conservancy[f]
	ANA03	*Aotus nancymaae*	Nancy Ma's owl monkey	M	f	DuMond Conservancy[f]
	ANA04	*Aotus nancymaae*	Nancy Ma's owl monkey	M	f	DuMond Conservancy[f]
	ANA05	*Aotus nancymaae*	Nancy Ma's owl monkey	M	f	DuMond Conservancy[f]
	ANA06	*Aotus nancymaae*	Nancy Ma's owl monkey	M	f	DuMond Conservancy[f]
NWP	CD01	*Callicebus donacophilus*	white-eared titi monkey	M	m	San Diego Zoo / CRES[e]
	CD02	*Callicebus donacophilus*	white-eared titi monkey	M	m	San Diego Zoo / CRES[e]
	CM01	*Callicebus moloch*	dusky titi monkey	M	m	NIA: NG06115[g]
	PP01	*Pithecia pithecia*	white-faced saki monkey	M?	m	San Diego Zoo / CRES[e]
	PP02	*Pithecia pithecia*	white-faced saki monkey	M?	f	San Diego Zoo / CRES[e]
	SS01	*Saimiri sciureus*	squirrel monkey	P, PG	m	San Diego Zoo / CRES[e]
	SS02	*Saimiri sciureus*	squirrel monkey	P, PG	f	San Diego Zoo / CRES[e]
	SS03	*Saimiri sciureus*	squirrel monkey	P, PG	f	NG05311[g]
	CG01	*Callitrhix geoffroyi*	white-fronted marmoset	M, PG, PA	f	PR01094[h]
	CJ01	*Callithrix jacchus*	marmoset	M, PG, PA	m	calJac3[i]
	SF01	*Saguinus fuscicollis*	white-lipped tamarin	PA	f	NG05313[g]
	LL01	*Lagothrix lagotricha*	woolly monkey	P	f	NG05356[g]
OWP	OG01	*Otolemur garnettii*	bushbaby	S	?	Ensembl:GCA_000181295.3[j]
	EP01	*Erythrocebus patas*	patas monkey	PG	f	NG06116[g]
	RM01	*Macaca mulatta*	rhesus macaque	PG	f	NG06249[g]
	RM02	*Macaca mulatta*	rhesus macaque	PG	f	rheMac2[i]
	PAP01	*Papio anubis*	olive baboon	PG	m	PR00036[h]
APE	NL01	*Nomascus (Hylobates) leucogenys*	white-cheeked gibbon	M, PGA	m	PR01038[h]
	NL02	*Nomascus leucogenys*	white-cheeked gibbon	M, PGA	f	NLeu1.0[i]
	HSY01	*Hylobates syndactylus*	siamang	M, PGA	f	PR00969[h]
	PA01	*Pongo pygmaeus abelii*	orangutan	S	m	PR00253[h]
	PA02	*Pongo pygmaeus albeii*	orangutan	S	f	ponAbe2[i]
	GG01	*Gorilla gorilla*	gorilla	PG, PA	f	gorGor3[i]
	PP01	*Pan paniscus*	bonobo	PGA	f	PR00092[h]
	PT01	*Pan troglodytes*	chimpanzee	PGA	f	PR00605[h]
	PT02	*Pan troglodytes*	chimpanzee	PGA	m	panTro2[i]
Homo sapiens	HS01[m]	*Homo sapiens*	human	M, PG, PA	m	Promega G304A[k]
	HS02[m]	*Homo sapiens*	human	M, PG, PA	m+f	hg19[i]
	ASW	*Homo sapiens*	human	M, PG, PA	37f, 24m	African Americans in SW USA[l]
	LWK	*Homo sapiens*	human	M, PG, PA	48f, 47m	Luhya in Webuye, Kenya[l]
	YRI	*Homo sapiens*	human	M, PG, PA	45f, 43m	Yoruba in Ibadan, Nigeria[l]
	CLM	*Homo sapiens*	human	M, PG, PA	31f, 29m	Colombians from Medellin, Colombia[l]
	MXL	*Homo sapiens*	human	M, PG, PA	34f, 30m	Mexican Ancestry in Los Angeles USA[l]
	PUR	*Homo sapiens*	human	M, PG, PA	27f, 28m	Puerto Ricans from Puerto Rico[l]
	CHB	*Homo sapiens*	human	M, PG, PA	53f, 44m	Han Chinese in Beijing, China[l]
	CHS	*Homo sapiens*	human	M, PG, PA	50f, 50m	Southern Han Chinese[l]
	JPT	*Homo sapiens*	human	M, PG, PA	39f, 50m	Japanese in Tokyo, Japan[l]
	CEU	*Homo sapiens*	human	M, PG, PA	40f, 45m	Utah Residents European ancestry[l]
	FIN	*Homo sapiens*	human	M, PG, PA	58f, 35m	Finnish in Finland[l]

(*continued on next page*)

Table 1 (*continued*)

Clade	ID	Species	Common Name	Mating System[a]	Sex	Source / Accession / Build
	GBR	*Homo sapiens*	human	M, PG, PA	48f, 41m	British in England and Scotland[l]
	IBS	*Homo sapiens*	human	M, PG, PA	7f, 7m	Iberian population in Spain[l]
	TSI	*Homo sapiens*	human	M, PG, PA	48f, 50m	Toscani in Italia[l]
Rodent	MM01	*Mus musculus*	mouse	PG	m+f	mm10[i]
	RN01	*Rattus norvegicus*	rat	PG	m+f	rn04[i]

[a] Mating system code (follows mating system descriptions found in Mitani et al., 2012): M: monogamy, PGA: polygynandry, PG: polygyny, PA: polyandry, S: solitary/noyau.
[b] *A. azarae* control sample AAPLunk was sequenced and used in both phylogenetic and population genetic analysis of *OXTR*.
[c] Wild caught in Formosa Province, Argentina (Lat: 25°, 59.4 min S; Long: 58°, 11.0 min W, see Babb et al., 2010 for details).
[d] Zoológico de Sáenz Peña, Sáenz Peña, Chaco Province, Argentina.
[e] San Diego Zoo / CRES, San Diego, California, USA.
[f] DuMond Conservancy, Miami, Florida, USA.
[g] NIA sample archive, Coriell Institute, Camden, New Jersey, USA.
[h] IPBIR sample archive, Coriell Institute, Camden, New Jersey, USA.
[i] UCSC Genome Browser (Kent et al. 2002; Karolchik et al. 2014): http://genome.ucsc.edu.
[j] Ensembl Genome Browser (Flicek et al. 2011): http://www.ensembl.org.
[k] Control human genomic DNA G304A (Cat. # G3041), Promega Corporation, Madison, Wisconsin, USA.
[l] 1000 Genomes Project Server (1000 Genomes Project Consortium 2010, 2012): ftp://ftp-trace.ncbi.nih.gov/1000genomes/ftp/.
[m] Human samples HS01 and HS02 were sequenced and used in the phylogenetic analysis of *OXTR*, but were not included in the population genetic analysis.

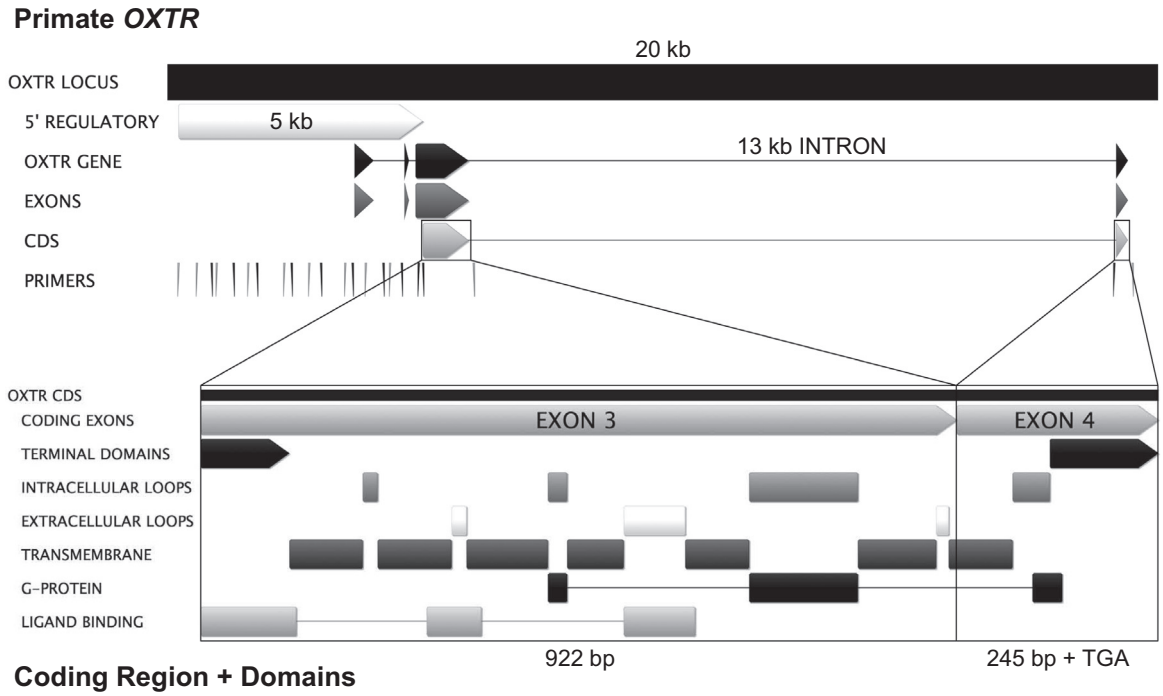

Fig. 1. A diagram of the *OXTR* genetic locus, constructed from the consensus alignment of seven publicly available primate genome sequences. See Table 1 for sequence codes and references. A schematic diagram of the *OXTR* locus (20 kb window), shown 5′–3′ from left to right at the top of the figure, is followed by a zoom (1200 bp window) of the coding region underneath. Both figures exhibit tracks beneath them that depict major structural regions of the gene. In the 20 kb window, the 5′ regulatory region, the coding region (CDS), and the two coding exons (exons 3 and 4) are shown in shades of *gray*. Below, the locations of the oligonucleotide primers used in this study for PCR amplification are shown in their approximate positions and depicted as *dark gray* (F) and *black* (R) triangles. In the zoomed 1200 bp window, the two coding exons are shown adjacent to one another, and the different protein-coding domains of the *OXTR* gene are depicted as tracks in shades of *gray* below.

most frequent *OXTR* coding haplotype (and most common mtDNA haplotype; see Babb et al., 2011a). We aligned the *A. azarae* sequence with the other 38 primate and rodent *OXTR* coding sequences using Geneious Pro, and organized *OXTR* 5′ regulatory region, CDS, and protein domain (ligand binding, G-protein binding, and transmembrane domain) MSAs. We then formatted and annotated all matrices in Geneious Pro v.5.6.7 for calculations in PAUP* 4.0b10 (Swofford, 2002), PAML/codeML (Yang, 2007), and MrBayes (Huelsenbeck et al., 2001; Huelsenbeck and Ronquist, 2001; Ronquist and Huelsenbeck, 2003).

2.5.2. Interspecific summary statistics

In line with our intraspecific analyses, we generated summary statistics for the phylogenetic data sets containing the 5′ regulatory region, CDS and protein domain region MSAs using Geneious Pro and R (pegas and ape packages). We measured overall pairwise identity and nucleotide diversity (π) for each MSA to estimate overall alignment variation. We also investigated all segregating sites and recorded GC content, transitions (TI), transversions (TV), and insertion/deletions for all alignments, and noted any putative amino acid substitutions for the CDS and protein-domain MSAs.

Table 2
Primer sequences designed and optimized for *OXTR* amplification and sequencing.

Genetic region	Oligo name	Strand	Sequence (5′–3′)
5′ Regulatory region (overlapping coverage)	Reg01-F	Forward	GAA CGC ACC CTC CAT GAC CC
	Reg01-R	Reverse	CAC CGA AGC AGG TAC TGT GGA
	Reg02-F	Forward	TTC CTC CGG GAC TGG GAA TC
	Reg02-R	Reverse	ATT CCA ACC GAG GCT CCA GA
	Reg03-F	Forward	AAC GTT CGG GAA ACC TCG AC
	Reg03-R	Reverse	CTG GAG GTG TGG GAG GAG AG
	Reg04-F	Forward	CTG CAA GAG GGA AGG AAC TCG T
	Reg04-R	Reverse	GGA CTT GCC CAA GGT CAC TCC A
	Reg05-F	Forward	AGC CAA GGA CCA GGT TTC CT
	Reg05-R	Reverse	TTC CTG CCT GGT TTC TGC AC
	Reg06-F	Forward	AGC CTG TGA GAC AGC CTA ACT
	Reg06-R	Reverse	GGT ATC CAT GGG GGA CTG GT
	Reg07-F	Forward	TGC CAT GTG CCA ACT ACA AC
	Reg07-R	Reverse	ACT GAC CTC CCT CAG CAA GA
	Reg08-Fb	Forward	AGA TGG GGT GCC TGG AAG GAC T
	Reg08-Rc	Reverse	GGG AAC AAC ACA CAG TGG GG
	Reg09-F	Forward	TCT CAT GCA AAA ACA ACC TCA CAG A
	Reg09-Ra	Reverse	TGT CTT TTG ACC CAG CAA TCT C
Coding region (Exon 3)	Ex3-F2b	Forward	CCT ACA CCC TCC GAC AC
	Ex3-R3b	Reverse	GAC TCT GTG GGA TTT CAA AC
Coding region (Exon 4)	Ex4-F	Forward	TGC CCT TTT CTC CTT TCT CC
	Ex4-R	Reverse	CCT ACT GTA GCC ACC CCA AG

In addition, we explored the 5896 bp 5′ regulatory region MSA of eight primate species for repetitive elements, polyadenylation (poly(A)) sites, insertion and deletion events, and chromosomal rearrangements. We searched for sites underlying putative transcription factor binding sites (TFBS) using the transcription factor prediction (binding site threshold = 6 nucleotides) software plugin for Geneious Pro. To estimate the putative transcriptional start site (TSS) locations in the 8 interspecific 5′ regulatory sequences, we implemented the Eponine TSS prediction algorithm. This algorithm applies a hybrid machine-learning approach, pre-trained on the Eukaryotic Promoter Database, to identify eukaryotic promoters by assigning likelihood values to text string queries based on the structures of learned models such as canonical TATA box motifs and regions of C + G enrichment (Down and Hubbard, 2002). We further interrogated the Database of Genomic Variants (DGV) (Iafrate et al. 2004) for evidence of structural variation, such as copy number variants (CNVs) or segmental duplications, near *OXTR*. We conducted the above feature searches and annotated all findings using Geneious Pro.

2.5.3. Network analysis

We generated intraspecific multistate median joining (MJ) networks for all *A. azarae* 5′ regulatory and coding MSAs using Network v4.6.1.0 (Bandelt et al. 1999). We similarly produced a multistate amino acid MJ network for the phylogenetic MSA of *OXTR* coding sequences to explore the amino acid variation across broader evolutionary distances. To evaluate this level of molecular diversity, we translated the 1167 bp nucleotide sequences into 389 amino acid sequences for the set of 39 interspecific samples, and ran the resulting protein MSA in Network.

2.5.4. Phylogenetic model selection

To select the most appropriate model for our analyses, we ran the program jModelTest v2.1.1 (Guindon and Gascuel, 2003; Felsenstein, 2005; Darriba et al., 2012; Posada, 2008) using 203 substitutions patterns to survey 1624 models of nucleotide substitution (+F base frequencies, rate variation of +I and +G with nCat = 4). We implemented the Akaike Information Criterion (AIC) setting, and conducted parallel searches using Bayesian Information Criterion (BIC) and performance-based Decision Theory (DT). The base tree for our likelihood calculations was optimized for Maximum Likelihood (ML) phylogenetic analyses.

2.5.5. Maximum likelihood and Bayesian inference analyses

We conducted ML analysis in PAUP* v4.0b10 (Swofford, 2002) to estimate the most likely evolutionary tree based on the alignments of *OXTR* nucleotides and amino acid codons using the nucleotide model specified by jModelTest. For ML analysis, we estimated bootstrap values based on a set of 10,000 replicates. To recover the phylogenetic tree (or set of trees) that maximized the probability of obtaining our data given a specified model of evolution, we undertook Bayesian inference analysis (BI) with the software program MrBayes v3.1.2 (Huelsenbeck and Ronquist, 2001; Huelsenbeck et al., 2001; Ronquist and Huelsenbeck, 2003). In the BI analysis, we used the ML function and employed the BIC-specific nucleotide substitution model suggested by jModelTest. The Markov Chain Monte Carlo (MCMC) search was run with four chains for 1,000,000 generations, with trees sampled every 1000 generations. To ensure the accuracy of our MCMC search, we assessed the average standard deviation in split frequencies among the four chains, and accepted a construction when the level chain deviation reached <0.05. We discarded the first 5000 trees as "burn-in" to remove extraneous pre-convergence probability values that can skew the architecture of a given consensus Bayesian tree (Huelsenbeck et al., 2001; Altekar et al., 2004).

2.5.6. Analysis of adaptive evolution

We conducted ML analysis in PAUP* 4.0b10 to estimate the most likely gene tree based on the alignments of *OXTR* nucleotides and amino acid codons and using the nucleotide substitution model(s) specified by jModelTest. To investigate signatures of selection along phylogenetic branches, we next analyzed the ratio of non-synonymous (d_N) to synonymous (d_S) amino acid changes for *OXTR* mRNA and domain-specific regions independently using the topology of the ML gene tree. We then used the codeML program within PAML to calculate the relative rates of change along different phylogenetic branches. We subsequently applied a likelihood ratio test (LRT) to estimate the accuracy ranges of two phylogenetic models, M0 (variable branch lengths/substitution rates) and M1 (homogeneous branch lengths/substitution rate).

2.5.7. Bayesian coalescent estimation

To map the *OXTR* mutation rate within the primate phylogeny, we imported the 39-sequence *OXTR* coding region alignment into the annotation program BEAUti v1.5.4 for analysis in the program BEAST v1.5.4 (Drummond et al., 2006; Drummond and Rambaut, 2007). We set temporal priors based on log-normally distributed radiometric fossil dates to approximate coalescent ages of primate taxa (priors and groups outlined in Babb et al., 2011a, 2013). BEAST accounts for errors associated with a fixed mutation rate through Bayesian MCMC calculation of aligned molecular sequences (Ho et al., 2005) using calibrated paleontological events as priors (Drummond et al., 2002; Drummond and Rambaut, 2007).

We implemented Yule speciation process parameters with a relaxed lognormal molecular clock model, three partitions for codon positions, equal base frequencies, and ran BEAST using the nucleotide model specified by our jModelTest runs for 4,000,000 generations, echoing on-screen every 10,000 and logging every 200 generations. We assessed the level of convergence (<0.05) using the mean standard deviation in split frequencies among the four chains before accepting the post-convergence tree likelihoods of our runs. We then analyzed the Bayesian coalescent results with the companion software in TRACER v1.5 (Rambaut and Drummond, 2007) to view the distribution of coalescent time estimates and evaluate their accuracy based on the effective sample sizes (ESS) of the data. Finally, we summarized the 10,001 trees retained from BEAST in TreeAnnotator v1.5.4, and displayed in the program FigTree v1.4.2 (Drummond and Rambaut, 2007; Rambaut, 2014).

Table 3
Intraspecific summary statistics for *A. azarae* and *H. sapiens OXTR* sequences.

A. azarae (n=25)	5′ Regulatory	CDS[b]	Ligand binding[c]	G-protein binding[d]	Trans- membrane[e]
Nucleotides (bp)	4936	1167	270	192	600
GC content (% non-gap)	47.6%	63.7%	69.3%	69.3%	60.7%
Polymorphic sites	6	3	0	0	1
Transitions (TI)	5	1	0	0	0
Transversions (TV)	1	2	0	0	1
Insertion/deletions (indels)	0	0	0	0	0
Pairwise identity (%)	99.96%	99.70%	100.00%	100.00%	99.90%
Nucleotide diversity (π)	0.0005	0.0011	0	0	0.0009
Tajima's D (p)	1.20 (0.23)	1.43 (0.15)	NaN	NaN	1.56 (0.12)
Single nucleotide polymorphisms	314 C→G, 0.04	819 T→A, 0.34	–	–	819 T→A, 0.34
Consensus → putative derived, MAF[a]	1250 A→G, 0.02 2537 G→A, 0.30 3213 C→T, 0.30 3456 A→G, 0.24 4319 G→A, 0.32	1055 T→C, 0.08,[h] 1119 G→C, 0.26			
Putative non-synonymous substitutions	–	1	0	0	0
H. sapiens (n=1092)	5′ Regulatory	CDS[b]	Ligand binding[c]	G-protein binding[d]	Trans- membrane[e]
Nucleotides (bp)[f]	5325	1167	270	192	600
GC content (% non-gap)	46.5%	65.2%	71.5%	71.4%	62.7%
Polymorphic sites	88 (46[g])	18 (5[g])	0	3 (1[g])	9 (4[g])
Transitions (TI)	61	12	0	3	5
Transversions (TV)	27	6	0	0	4
Insertion/deletions (indels)	0	0	0	0	0
Pairwise identity (%)	99.80%	99.90%	100.00%	99.80%	99.90%
Nucleotide diversity (π)	< 0.0001	< 0.0001	0	< 0.0001	< 0.0001
Tajima's D (p)	−2.61 (0.009)	−1.58 (0.11)	NaN	−0.81 (0.42)	−1.46 (0.11)
Single nucleotide polymorphisms	**Supplementary Table 1**, 0.0005-0.85	171 C→T, 0.68	–	690 C→T, 0.24	171 C→T, 0.68
Consensus → alternate allele, alt. AF[a]		351 C→T, <0.01 360 G→T, <0.01 510 G→T, <0.01 515 T→C, 0.02,[h] 616 C→G, 0.01,[h] 652 G→A, 0.15,[h] 661 G→A, <0.01[h] 690 C→T, 0.24 700 A→G, <0.01,[h] 712 G→A, 0.01,[h] 963 C→A, <0.01,[h] 999 G→A, <0.01 1001 G→A, <0.01,[h] 1068 C→A, <0.01,[h] 1104 G→A, <0.01 1121 G→A, <0.01,[h] 1126 C→G, <0.01,[h]		700 A→G, <0.01,[h] 712 G→A, 0.01,[h]	351 C→T, <0.01 360 G→T, <0.01 510 G→T, <0.01 515 T→C, 0.02, [h] 616 C→G, 0.01, [h] 652 G→A, 0.15, [h] 661 G→A, <0.01[h] 963 C→A, <0.01,†
Putative non-synonymous substitutions	–	11	0	2	5

[a] Alternative allele frequency, with all alleles extracted from minus (−) strand.
[b] Alignment based upon human gene NM_000916 (Kent, 2002; Karolchik et al., 2014), with the terminal stop codon removed.
[c] Ligand binding domain denoted here as codon positions 1–39, 93–114, and 173–201 (Chini et al., 1997; Gimpl and Fahrenholz, 2001; Wesley et al., 2002).
[d] G-protein binding domain denoted here as codon positions 142–149, 224–267, with 339–350 being necessary for $G_{q/11}$ binding (Chini et al., 1997; Gimpl and Fahrenholz, 2001; Wesley et al., 2002).
[e] Transmembrane domain denoted here as codon positions 37–66 (TM1), 73–102 (TM2), 109–141 (TM3), 150–172 (TM4), 198–223 (TM5), 268–299 (TM6), and 305–330 (TM7) (Isberg et al., 2014; GPCRDB.org: SwissProt OT-R, human).
[f] Equivalent region used in the interspecific analyses, but with alignment gaps removed.
[g] Indicates number of polymorphic sites after the removal of positions that lack individuals that are homozygous for the alternate (non-reference) allele.
[h] Polymorphic site leading to a non-synonymous amino acid substitution.

2.6. Ethics statement

The work described in this article was conducted in accordance with EU Directive 2010/63/EU for animal experiments and with approval from the IACUC Committee at the University of Pennsylvania.

3. Results

3.1. Population genetic analyses

3.1.1. A. azarae intraspecific alignment summary

Our analysis of the *OXTR* 5′ regulatory and coding sequences revealed low levels of diversity. We identified six single nucleotide polymorphisms (SNPs) across the nearly 5 kb of the 5′ regulatory region of *OXTR* that was sequenced (Table 3). Four of these SNPs were found at high allele frequencies (24–32%), whereas two of them occurred as heterozygotes in only one or two of the individuals. None of the intraspecific regulatory variants led to putative transcription factor binding site (TFBS) changes. The nucleotide diversity (π) estimate for the 5′ regulatory region was extremely low (0.0005), with 99.96% pairwise identity between any two sequences. The slightly positive value for the selective neutrality index Tajima's D (1.20, $P = 0.23$) likely reflected a mix of high and low frequency variants at this locus, although this value was statistically non-significant (Table 3).

Our analysis of the 25 *OXTR* coding sequences also revealed a low level of diversity. We observed three SNPs at frequencies of 8%, 26%, and 34% (of 50 chromosomes) (Table 3). Within a wider sampling of the larger population ($n = 111$ individuals), these three SNPs were present at slightly higher frequencies (8%, 49%, and 65%; unpublished data). One of the three coding region SNPs was a transition (1055 T → C), whereas the other two were transversions (819 T → A and 1119 G → C). None of the coding SNPs produced non-synonymous amino acid substitutions, and only one occurred within a previously defined protein domain (819 T → A within the transmembrane domain). Neither the ligand-binding domain nor the G-protein domain of *A. azarae OXTR* CDS contained a single polymorphic site.

As observed in the *A. azarae* 5′ regulatory MSA, the nucleotide diversity (π) estimate for the CDS was low (0.0011), with 99.7% pairwise identity between any two sequences. Like the 5′ regulatory region, the CDS also had a slightly positive value for the Tajima's D index (1.43, $P = 0.15$), which was also statistically non-significant (Table 3). Interestingly, while the 5′ regulatory region contained a greater number of intraspecific SNPs (6 in 4936 bp), the coding region contained a higher proportion of intraspecific SNPs relative to sequence length (3 in 1167 bp).

3.1.2. H. sapiens intraspecific alignment summary

Our parallel analysis of *H. sapiens OXTR* 5′ regulatory and coding sequences revealed slightly higher levels of diversity than observed in *A. azarae*, although this finding is likely attributable to the much larger sampling of individuals in the human relative to the owl monkey population (1092 vs. 25). We recorded 88 SNPs across the nearly 5325 bp of 5′ regulatory region sequence alignment (Table 3, Supplementary Table 1). MAF values for these SNPs varied from rare (0.05) to very common (0.85). The nucleotide diversity (π) estimate for the 5′ regulatory region was <0.0001 ($P = 0$), with 99.8% pairwise identity between any two sequences. The Tajima's D index (−2.16, $P = 0.009$) for *H. sapiens* 5′ regulatory sequences was similar to that for *A. azarae*, with a mix of high and low frequency variants and a statistically non-significant value (Table 3). We note that these calculations ignore sites with only heterozygous genotype calls (e.g., an individual heterozygous "C/T" at a position receives an IUPAC call "Y"), indicating that our results likely underestimated the total number of variants present.

Even taking this into account, *H. sapiens OXTR* coding sequences revealed higher levels of diversity than expected. We observed 18 SNPs at frequencies ranging from <0.01 to 0.68, although the majority were singletons (Table 3). Twelve of the coding region SNPs were transitions and six were transversions. Surprisingly, 11 of the 18 *H. sapiens* coding SNPs led to non-synonymous amino acid substitutions, although all of them appeared at frequencies of 0.02 or lower (Table 3). Two non-synonymous substitutions occurred within the G-protein domain, and five in the transmembrane domain. As with the Azara's owl monkeys, the ligand-binding domain of the *H. sapiens OXTR* locus contained zero

Table 4
Interspecific summary statistics for primate ($n = 37$) and rodent ($n = 2$) *OXTR* sequences.

	5′ Regulatory[a]	CDS[b]	Ligand binding[c]	G-protein binding[d]	Trans-membrane[e]
No. of individuals (N)	8	39	39	39	39
No. of species and subspecies	8	25	25	25	25
Nucleotides (bp)[f]	5896	1167	270	192	600
GC content (% non-gap)	41.5%	64.0%	69.2%	68.8%	61.5%
Identical sites	3882	845	179	125	474
Non-identical sites	2014	322	90	67	126
Transitions (TI)	528	178	45	26	82
Transversions (TV)	276	74	26	18	26
Sites with TI + TV (+indels)	1210	70	19	23	18
Insertion/deletions (indels)	1156	3[g]	0	3[b]	0
Pairwise identity (%)	87.6%	94.8%	94.1%	93.6%	96.2%
Nucleotide diversity (π)	0.0629	0.0522	0.0595	0.0638	0.0387
Variable amino acid sites	–	77 (19.9%)	29 (32.2%)	19 (29.7%)	17 (8.5%)

[a] 5896 bp 5′ regulatory region alignment (including gaps) based on 8 primate sequences, including *A. azarae* sequence and genomic sequence extractions from HS02, GG01, PT02, NL02, PAB02, RM02, and CJ01 (Kent 2002; Kent et al., 2002; Karolchik et al., 2014).

[b] Alignment based upon human gene NM_000916 (Kent 2002; Karolchik et al., 2014), with the terminal stop codon removed. The minimum sequence length was 1164 bp (388 amino acids) belonging to MM01 and RN01, whereas the *OXTR* CDS sequences for all primate taxa were 1167 bp (389 amino acids) in length.

[c] Ligand binding domain denoted here as codon positions 1-39, 93-114, and 173-201 (Chini et al., 1997; Gimpl and Farenholz, 2001; Wesley et al., 2002).

[d] G-protein binding domain denoted here as codon positions 142-149, 224-267, with 339-350 being necessary for $G_{q/11}$ binding (Chini et al., 1997; Gimpl and Farenholz, 2001; Wesley et al., 2002).

[e] Transmembrane domain denoted here as codon positions 37-66 (TM1), 73-102 (TM2), 109-141 (TM3), 150-172 (TM4), 198-223 (TM5), 268-299 (TM6), and 305-330 (TM7) (Isberg et al., 2014; GPCRDB.org: SwissProt OT-R, human).

[f] Equivalent region used in the intraspecific analyses, but with all alignment gaps retained.

[g] The 3 nucleotide indels constitute a rodent-specific 3 bp deletion of codon 253, as observed in MM01 and RN01.

polymorphic sites. The nucleotide diversity estimate (π) for the *H. sapiens* CDS was <0.0001 ($P = 0$), with 99.9% pairwise identity between any two sequences. In contrast to other estimates of the Tajima's D index, there was a low negative value (−1.58, $P = 0.11$) indicative of an excess of low frequency variants (Table 3).

3.2. Phylogenetic analyses

3.2.1. Interspecific alignment summary

The interspecific analysis of primate and rodent *OXTR* 5′ regulatory and coding sequences revealed extensive diversity in the different regions of the locus and across different evolutionary lineages. Within the 5896 bp of the 5′ regulatory region MSA of eight haplorhine primate species, only 3882 sites were shared across all taxa (Table 4). This extent of sequence variation was further reflected by a pairwise identity value of 87.6% and a nucleotide diversity (π) value of 0.0629, making the interspecific 5′ regulatory region MSA the least conserved sequence alignment in the study.

Contributing to the variability of 5′ regulatory sequences was a >250 bp insertion in *Homo sapiens*, an orthologous >80 bp insertion in *Pan troglodytes*, and a distinct ~1000 bp insertion in only *P. troglodytes* (Fig. 2). Each of two orthologous insertions (~5500 bp upstream of the ATG start site) was characterized by the presence of a large number of repetitive dinucleotide "A + T" motifs, whereas the *P. troglodytes*-specific insertion (~3100 bp upstream of ATG) featured >480 bp of non-repetitive non-coding sequence and a 500 bp genomic contig gap. The ambiguous genomic gap sequence was trimmed from the MSA. By contrast, the 5′ regulatory sequences of the investigated NWP (*A. azarae* and *Callithrix jacchus*) were characterized by 10 shared deletions of >5 bp. Although one such NWP deletion (31 bp in length) was located 61 bp upstream from the putative TSS (positions 4455–4466 in the regulatory MSA), it did not appear to overlap this region. Moreover, the putative TSS was conserved in all eight samples and supported by human EST data from the UCSC GB (Karolchik et al., 2014).

In addition, we noted that the 5′ regulatory region for the two socially monogamous primates we examined (*A. azarae* and *Nomascus leucogenys*) exhibited substantial differences between them, with only 4437 of 5115 bases in a direct pairwise alignment

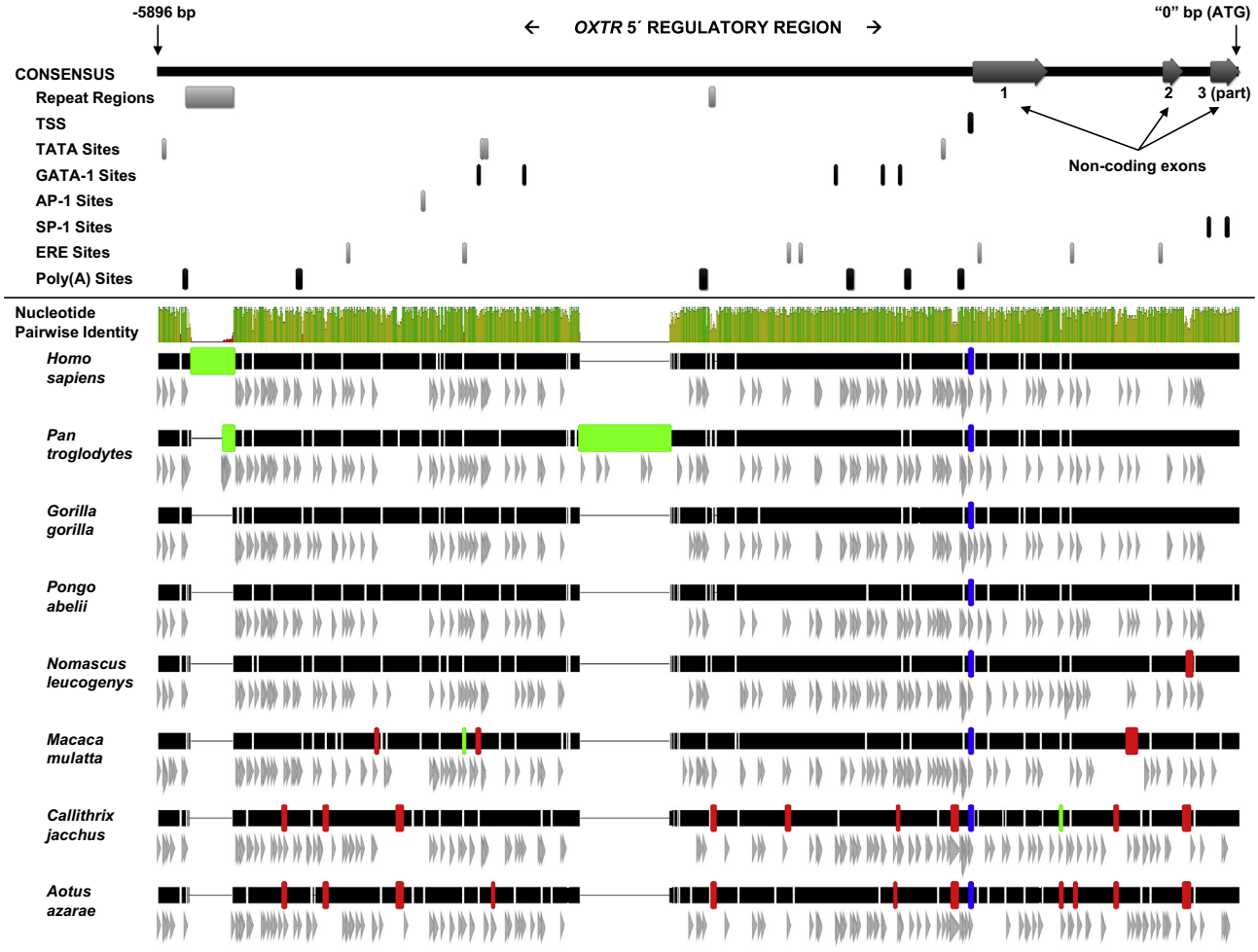

Fig. 2. A diagram showing sequence variation in the 5′ regulatory region of the *OXTR* gene in eight haplorhine primate species. Base numbering runs left to right, 5′–3′, from −5896 bp to 0, with the "MET" start codon (ATG) of the first coding exon (exon 3) occurring immediately following base 0. Panel a: (TOP) Notable landmarks across the 5′ regulatory region are depicted as tracks beneath a common consensus sequence, including repetitive regions, transcriptional start site (TSS) predicted by Eponine, putatively functional regulatory and transcriptional elements such as TATA box motifs, GATA-1 motifs, activator protein-1 and -2 (AP-1, AP-2) binding sites, specificity protein-1 binding sites, estrogen response element (ERE) binding sites, and potential polyadenylation (poly(A)) cleavage sites. Panel b: (BOTTOM) Alignment of 5′ regulatory region sequences of the *OXTR* gene in eight haplorrhine primate species, highlighting insertions and deletions >5 bp, and putative locations of mammalian transcription factor binding sites (TFBS) with lengths of 6 bp or more. Insertions are labeled in *green*, deletions in *red*, and TSS in *blue*. Both *Homo* and *Pan* feature insertions over 300 bp in size. Both NWP sequences (*Callithrix jacchus* and *Aotus azarae*) feature many deletions >5 bp, eight of which are shared between the two taxa. Transcription factor sequence recognition and binding sites (TFBS) are depicted as *gray* triangles beneath the sequences. (For interpretation of the references to color in this figure legend, the reader is referred to the web version of this article.)

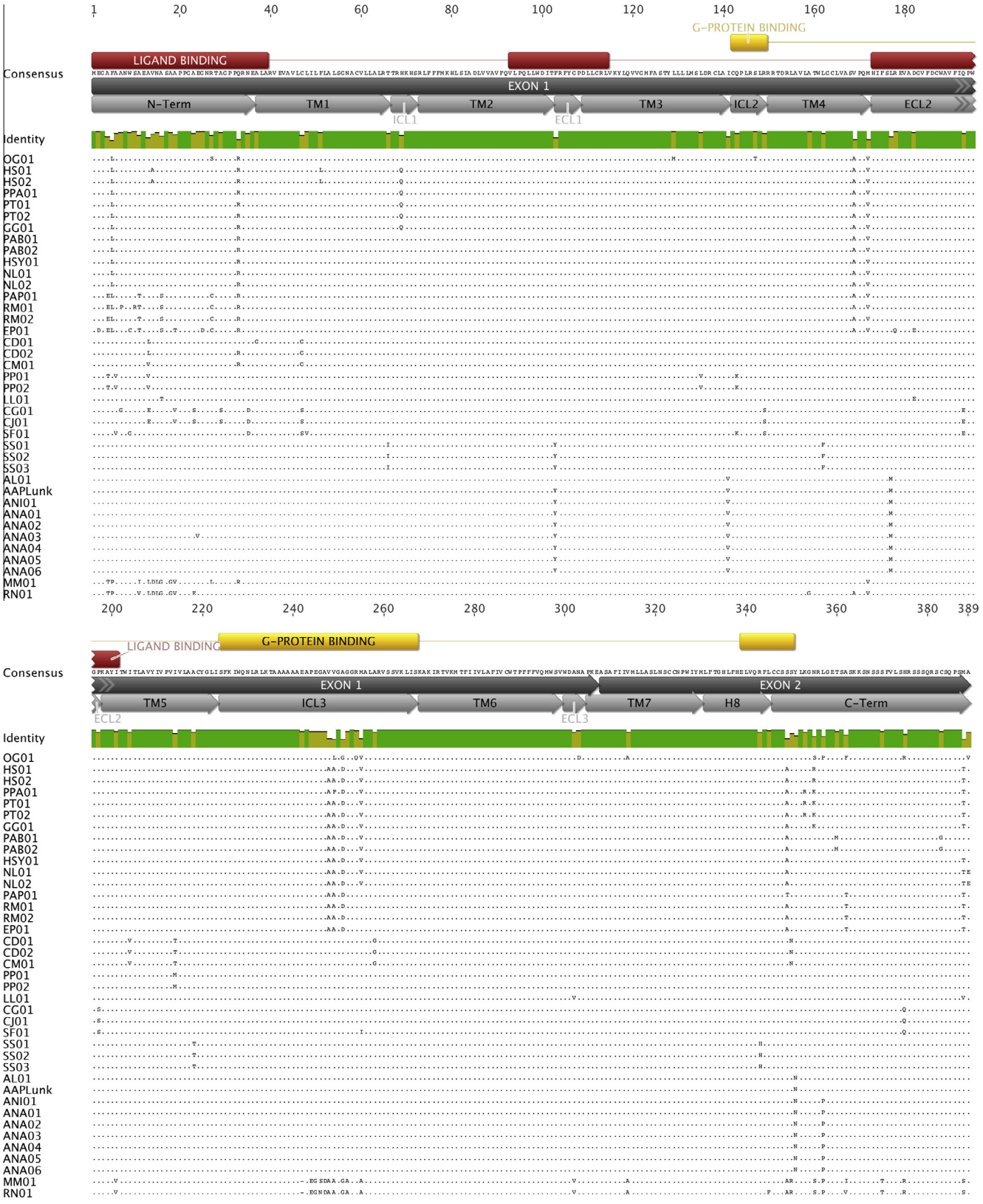

Fig. 3. A multisequence alignment of 39 *OXTR* amino acid sequences from 25 primate and rodent taxa. The full *OXTR* coding sequence (389 amino acid residues) is organized across two horizontal rows. The terminal, transmembrane, intracellular, extracellular, ligand binding and G-protein binding domains are shown above pairwise identity histograms at the top of each of the two alignment rows.

being identical (86.7%). Multiple CNVs have previously been reported for the 5′ regulatory region in primate genomes (Pinto et al., 2007; Jakobsson et al., 2008; Gregory et al., 2009; Itsara et al., 2009; Kim et al., 2009; Shaikh et al., 2009; Karolchik et al., 2014), although cross-primate alignment nets displayed no breakpoints (fission/fusion events) of chromosomes in any of the

primates throughout their cytogenetic evolution. Nevertheless, the 5′ regulatory region of *OXTR* possesses extensive sequence variability of a functional non-coding region across primate and rodent genomes.

The interspecific alignment of 39 spliced *OXTR* coding sequences exhibited 94.8% pairwise identity, but with only 845 of the 1167 nucleotide positions (72.4%) remaining constant across all taxa, and overall nucleotide diversity (π) was 0.0522. When translated, the interspecific *OXTR* CDS MSA exhibited 77 of 389 amino acid positions (19.9%) that were variable. In one particular case, the mouse (*Mus musculus*) and rat (*Rattus norvegicus*) both had nucleotides 757–759 (codon number 252) absent from exon 3 of *OXTR* (Fig. 3). This codon is present in all primate species.

We observed interspecific amino acid substitutions in all *OXTR* protein domains (Table 4, Fig. 3). Surprisingly, the ligand binding domain exhibited the greatest number (29) and proportion (32.2%) of amino acid substitutions across primate and rodent lineages, whereas the same domain was completely free of polymorphisms in both the *A. azarae* and *H. sapiens* populations. At the same time, the transmembrane domain exhibited the fewest number (17) and proportion (8.5%) of amino acid substitutions in the interspecific comparison despite having shown a notable level of polymorphic variation in the intraspecific analyses.

By contrast, CDS sequences belonging to taxa from the genus *Aotus* exhibited three unique amino acid substitutions that distinguish them from all other primates (141 I → V, 177 L → M, 351 Y → N), and one amino acid position that was shared only with *Otolemur garnettii* and the two rodent samples (357 L → P). Of these *Aotus*-specific non-synonymous (d_N) amino acid changes, 141 I → V was located in the transmembrane domain, 177 L → M was observed to reside within the ligand binding domain, and both 351 Y → N and 357 L → P were situated at the end of the gene in the C-terminal domain (Fig. 3). Furthermore, 18 amino acid substitutions located in every domain of the mature protein distinguished the *A. azarae* from the *H. sapiens OXTR* CDS (Fig. 4).

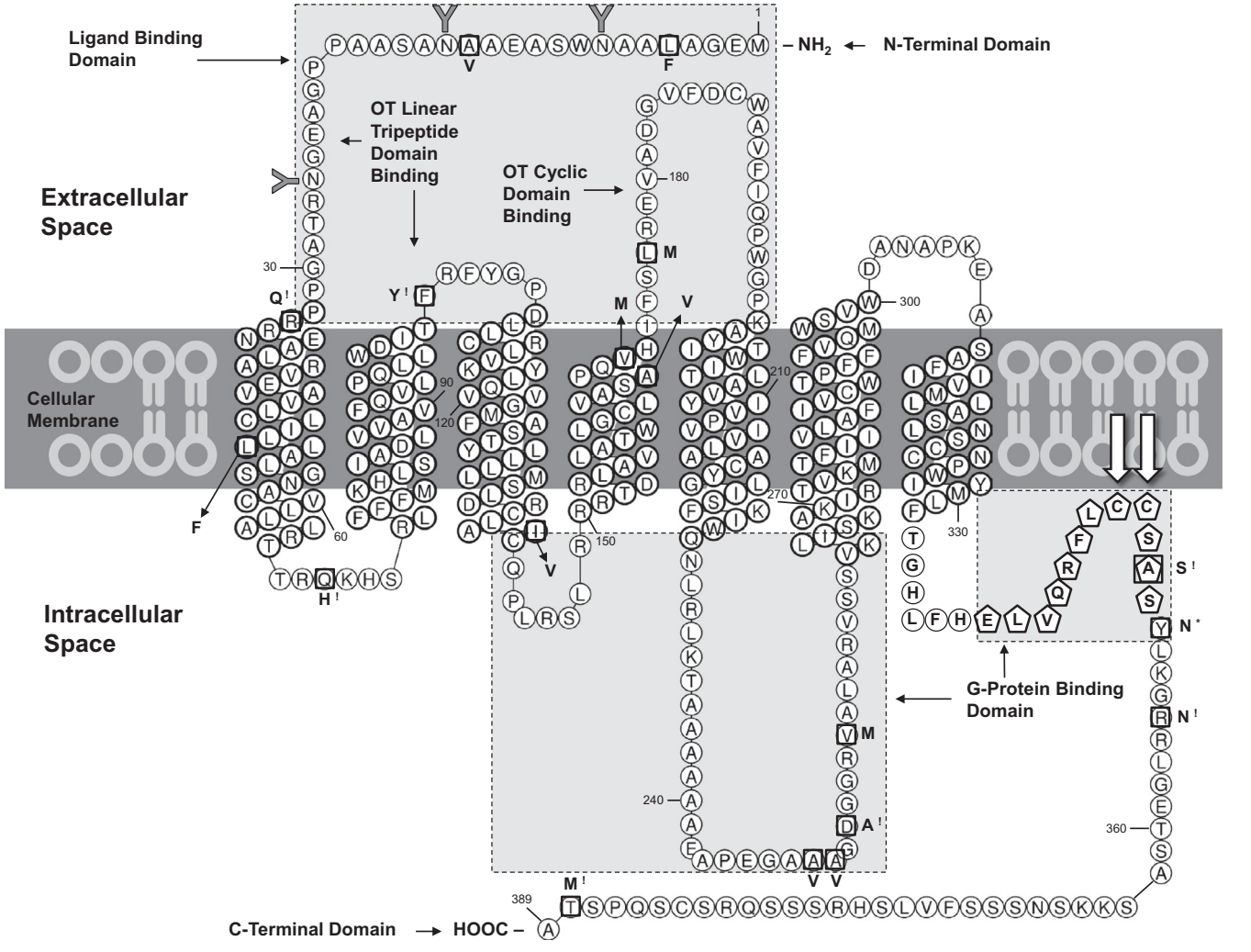

Fig. 4. A two-dimensional "snake-plot" diagram of *OXTR* amino acid sequence projected onto the mature OXTR receptor protein molecule structure. The amino acid sequence is based on human gene sequence NM_000916, with the terminal stop codon removed (389 amino acid residues, SwissProt OT-R, human, GPCRDB.org). The amino acid sequence is numbered every 30 residues. *A. azarae* amino acid changes (relative to the *H. sapiens* sequence) are depicted as *black* squares surrounding specific circular residue symbols. Residues that are marked with exclamation points (!) beside them indicate that they differ between *A. azarae* and *H. sapiens* with the difference implying a shift in hydrophobicity, whereas residues with asterisk (*) markings indicate that the amino acid substitution at that position implies a change in isoelectric point. The pentagonal boxes highlight the amino acid residues that are functionally necessary for G_q protein binding. "Y"-shaped *gray* block symbols at residues N8, N15, and N26 mark sites of putative N-glycosylation, and *white* block arrow symbols at residues C346 and C347 mark sites of putative palmitoylation. Ligand binding protein domain (codon positions 1–39, 93–114, and 173–201) and G-protein binding domain (codon positions 142–149, 224–267, 339–350) are shown in *gray* boxes (Chini et al., 1997; Gimpl and Fahrenholz, 2001; Wesley et al., 2002).

3.2.2. Network analysis

The MJ network of 25 *A. azarae* 5′ regulatory region sequences of the *OXTR* gene revealed six distinct haplotypes, defined by the six regulatory SNPs (Fig. 5a). The *OXTR* CDS network revealed six distinct haplotypes defined by the three exonic SNPs. Three of these haplotypes occurred at high frequencies in the population (Fig. 5b).

In the interspecific network of 39 *OXTR* amino acid sequences (389 amino acids), 42 amino acid substitutions separated the NWP from OWP and APES, which exhibited considerably less mutational substructure and shorter internal branch lengths than the NWP (Fig. 6a). Among the NWP, *Callicebus* spp. and *Pithecia pithecia* were differentiated from other NWP by the two shared, derived substitutions. By contrast, no amino substitutions were exclusively shared among *Aotus*, *Saimiri*, *Callithrix* and *Saguinus*, despite their established phylogenetic relationships (Perelman et al., 2011). Among the APES, *Pan troglodytes* and *Pan paniscus* were separated from *H. sapiens*, and all coalesced to the node occupied by *Gorilla gorilla* (which is not the true ancestral lineage of these taxa). This observation suggested that at least 3 *OXTR* amino acid substitutions, and possible other reversions, have occurred in the last ~10 million years of human–chimp–gorilla evolution (Prado-Martinez et al., 2013).

3.2.3. Phylogenetic model selection

The AIC model search run by jModeltest selected the HKY + G (gamma distribution) model (Hasegawa et al., 1985) with a likelihood score ($-\ln L$) of 4411.08. By contrast, the BIC and DT model searches chose the TPM2uf + I + G model (invariant sites + gamma), and both searches provided likelihood scores of $-\ln L = 4414.67$. Because of this discrepancy at the model selection phase, we applied both TPM2uf and HKY models in all subsequent phylogenetic analyses to evaluate any inconsistencies in the results, and detected no significant changes in the phylogenetic arrangements or branch lengths that were specific to one model or the other.

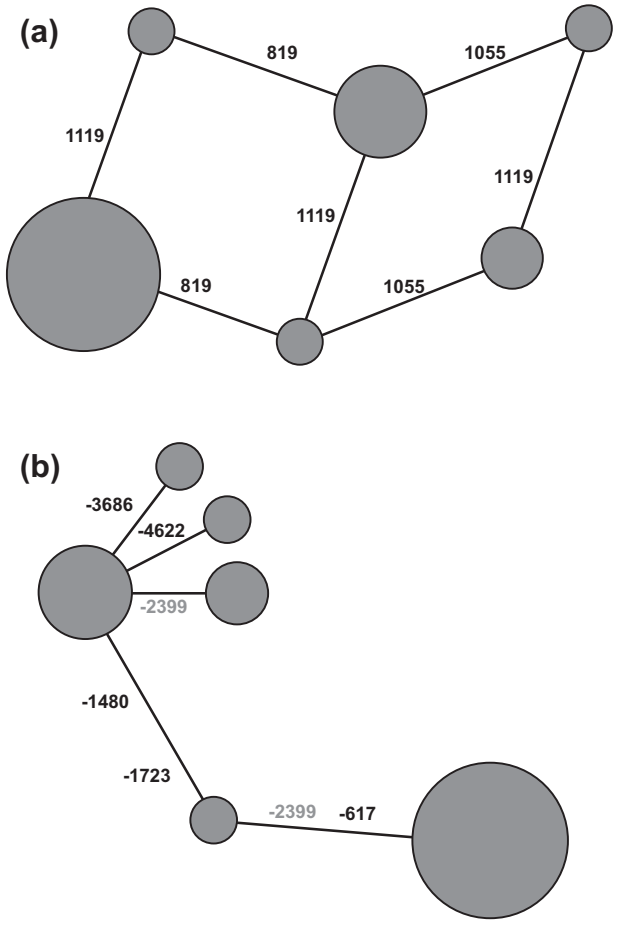

Fig. 5. Panel a: A median joining (MJ) network of *OXTR* 5′ regulatory region sequences from 25 *A. azarae* individuals. Six SNPs were detected in 4936 bp and defined six haplotypes. Node size is relative to the number of individuals that share a particular sequence. Panel b: A median joining (MJ) network of *OXTR* CDS region sequences from 25 *A. azarae* individuals. Three SNPs were detected in 1167 bp and defined six haplotypes. Node size is relative to the number of individuals that share a particular sequence.

3.2.4. Maximum likelihood and Bayesian inference analyses

In general agreement with our network analysis, the composite ML + BI tree (Fig. 6) exhibited a similar arrangement of taxonomic relationships as seen in other, more comprehensive analyses of genetic and genomic sequence data (Opazo et al., 2006; Poux et al., 2006; Hodgson et al., 2009; Wildman et al., 2009; Perelman et al., 2011). Nevertheless, the phylogenetic relationships among these taxa remained consistent across the different analyses that we performed, and ML bootstrap and BI posterior probability support values were high for all major phylogenetic branches. Among primates, the *Callithrix*/*Saguinus* clade possessed the greatest number of substitutions per site, and overall the NWP exhibited more nucleotide changes than the OWP or APE lineages.

3.2.5. Analysis of adaptive evolution

To detect signatures of adaptive evolution, we predicted the relative rates of *OXTR* amino acid changes along the different phylogenetic branches in disparate mammalian taxa using the ML tree calculations. The resulting d_N/d_S ratio values for the majority of branches were exceptionally low ($d_N/d_S = 0.0001$), suggesting that negative (purifying) selection may be maintaining the conservation of *OXTR* amino acid sequences in different primate lineages (Yang, 2007) (Fig. 6). We noted stronger positive selection signals ($d_N > d_S$) on branches leading to the broad taxonomic outgroups, such as those distinguishing the primate and rodent orders ($d_N/d_S = 7.0679$), although the power to accurately detect selected sites on this branch is likely limited by the small number of sequences (2) analyzed from the rodent clade. The LRT indicated that the M1 (variable) model was more likely ($-\ln L = 4292.53$) than the M0 (homogenous $d_N/d_S = 0.0546$ for the entire tree) model ($-\ln L = 4258.31$), although this result was statistically non-significant ($P > 0.8381$). Thus, to more finely partition *OXTR* amino acid substitution rates, we opted to report individual branch specific d_N/d_S estimates.

3.2.6. Bayesian coalescent estimation

The topology of the phylogenetic chronogram exhibited taxonomic arrangements similar to those seen in both the ML and median network analyses (Fig. 7). In addition, age estimations and their associated error ranges generated at each phylogenetic node were consistent with those of other recent studies of molecular data, although divergence estimates for the NWP and OWP were slightly younger than estimates from other studies (Hodgson et al., 2009; Perelman et al., 2011; Prado-Martinez et al., 2013). High mutation rates were evident for the branches extending from rodents to the primate clade, as well as those leading to the NWP, OWP, and the *Callithrix*/*Saguinus*/*Saimiri* clades.

4. Discussion

4.1. Owl monkey and human populations exhibit low intraspecific OXTR 5′ regulatory and coding variation

The overall intraspecific sequence variation present in the 5′ regulatory and coding regions of *OXTR* in *A. azarae* and *H. sapiens*

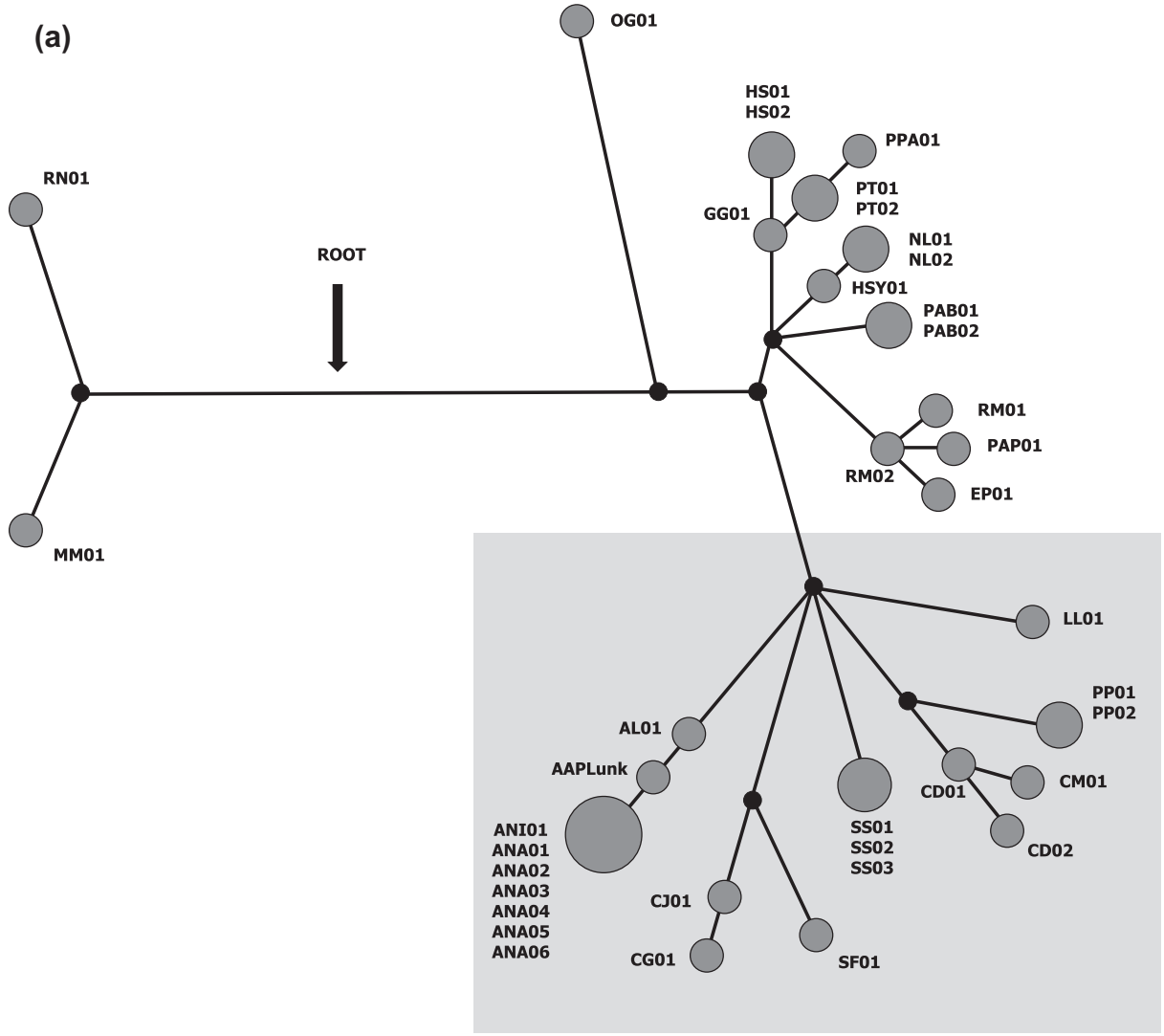

Fig. 6. Panel a: A MJ network of 39 *OXTR* amino acid sequences from 25 primate and rodent taxa. See Table 1 for sequence codes and references. The branches leading to the different clades are proportional to their actual mutation distances. Node size is relative to the number of individuals that share a particular sequence motif. The extent of mutational substructure of amino acid sequences is evident in the NWP clade, which is shown in a *gray* box. Panel b: A consensus phylogram representing the agreement of the ML and BI phylogenetic arrangements of 39 *OXTR* coding region sequences of 1167 bp representing 25 different mammalian species. Branch lengths display the relative number of mutational differences detected for each different taxonomic group. The d_N/d_S values are shown above each branch, and ML bootstrap values (of 10,000 replicates) appear below them. Posterior probabilities of the phylogenetic arrangement are displayed as a grayscale gradient across the taxa. Broad phylogenetic clade membership, drawn as *gray* vertical lines, is shown at the right. *Gray* stars next to taxon labels indicate that monogamy is the primary social system found in a particular taxon, whereas *white* stars indicate taxa in which some degree of monogamous social systems exists.

populations is limited. Of the 6103 bp surveyed in Azara's owl monkeys, only 9 polymorphic sites occur in 25 individuals. For the *H. sapiens* population, we observe 106 polymorphic sites in the 6492 bp surveyed in 1092 individuals, although the bulk of them are singletons (i.e., rare variants) and likely reflect the impact of recent demographic events (e.g., exponential population growth) experienced by human populations over the last 10,000 years (Keinan and Clark, 2012). Estimates of nucleotide diversity (π) and Tajima's *D* for both owl monkey and human populations suggest neutral or weak negative selection generally acting on the *OXTR* locus. One example at the extreme end of this trend may be the ligand-binding domain within the CDS, which exhibits a complete lack of polymorphism in both populations, suggesting that negative (purifying) selection may be promoting the functional conservation of this domain of the OXTR protein. This is not entirely surprising, seeing that SNP rates for the *OXTR* CDS in both humans and owl monkey populations are similar to those observed at another neuroendocrine receptor locus, the prolactin receptor gene (*PRLR*, Babb et al., 2013; Supplementary Table 2). In addition, pairwise nucleotide and amino acid comparisons of owl monkey and human *OXTR* coding sequences suggest that this locus has undergone less change than other loci we have investigated, including arginine vasopressin V1a (*AVPR1A*), another GPCR-coding gene (Supplementary Table 2).

4.2. NWP, OWP and APE clades exhibit high interspecific OXTR regulatory and coding variation

Our interspecific analyses of the *OXTR* locus reveal substantial variation in 5′ regulatory and coding sequences across primate lineages. This finding suggests that primates express OXTR proteins differently, and that the structure of OXTR proteins is functionally distinct in different primate taxa. Thus, while extant primate populations may exhibit low polymorphism levels at the *OXTR* locus, this was likely not the case throughout the evolution of different primate lineages.

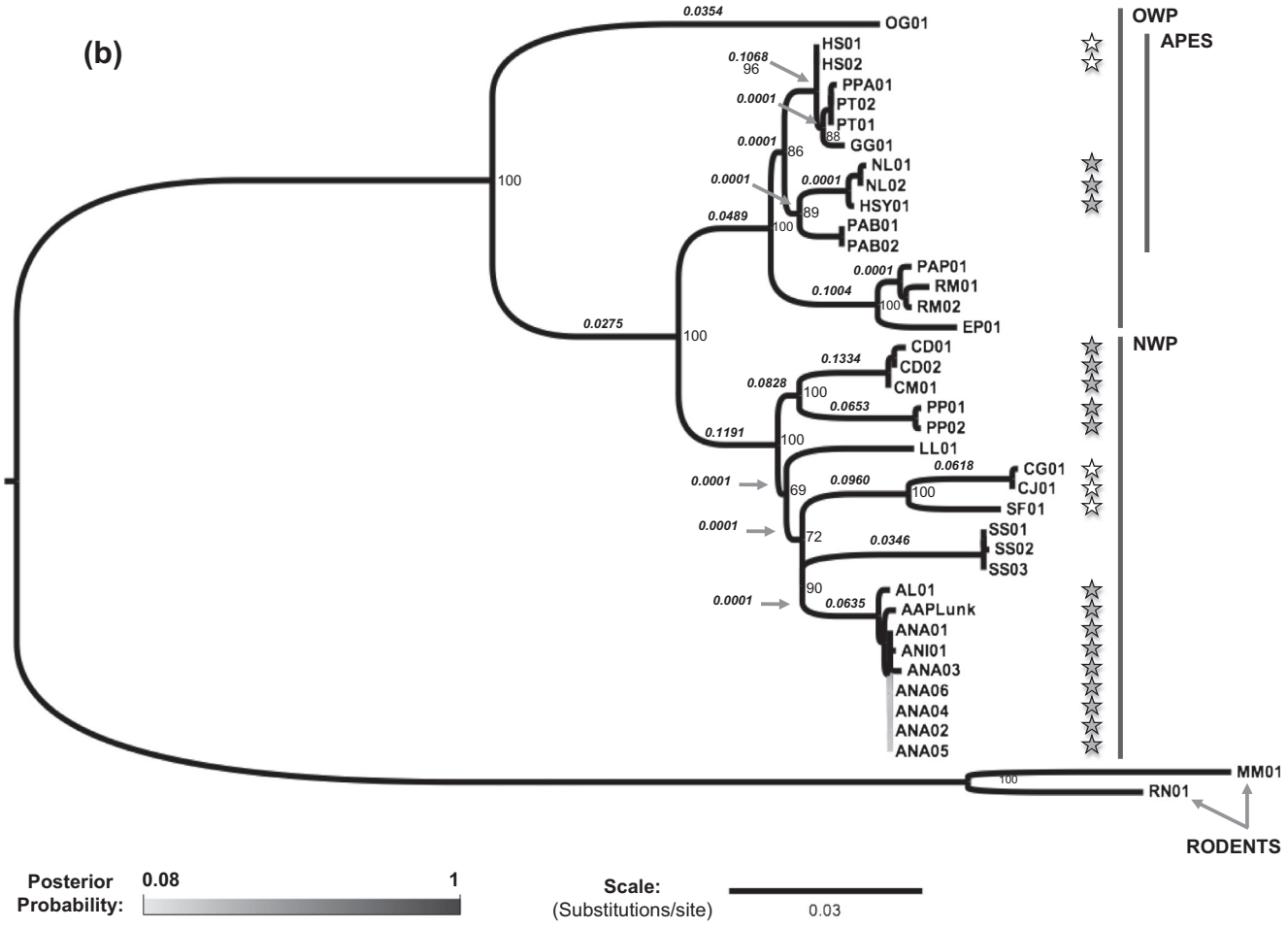

Fig. 6 (*continued*)

The 5′ regulatory region of *OXTR* in owl monkeys contains 144 putative TFBS, whereas the same region contains 138 TFBS in *Pongo pygmaeus abelii* sequences and 167 TFBSs in *P. troglodytes* (Fig. 2). Although the putative TSS is conserved across the eight interspecific 5′ regulatory region sequences that we examined, NWP sequences are characterized by many deletions of >5 bp, while the human (*H. sapiens*) and chimpanzees (*P. troglodytes*) sequences exhibit unique patterns of large motifs of dinucleotide A + T repeats ~5500 bp upstream of the *OXTR* coding sequence start site (ATG). The presence and absence of such transcriptionally relevant elements may act to enhance or insulate *OXTR* expression in NWP.

Despite the presence of numerous SNPs and insertion–deletions, it appears that major chromosomal rearrangements or structural variations have not completely reshuffled the 5′ regulatory region of the *OXTR* in different primates taxa, and the entire *OXTR* locus has retained chromosomal synteny throughout primate evolution (Fig. 2). Other studies have reported that, for humans, CNVs exist in the region (Pinto et al., 2007; Jakobsson et al., 2008; Gregory et al., 2009; Itsara et al., 2009; Kim et al., 2009; Shaikh et al., 2009). Simple repetitive elements (such as STRs and VNTRs), similar to those upstream of the *OXTR* locus in humans and chimps, may therefore influence the accumulation of more mutations or the formation of larger CNVs (Conrad et al., 2010). Thus, it is possible that the same properties that enable regulation of transcription may be mildly mutagenic for CNV formation, and as a result, such CNVs may affect the evolution of gene regulation (Conrad et al., 2010; Gökçumen et al., 2011; Iskow et al., 2012).

The coding region of *OXTR* is also extremely variable across primate taxa, with 322 of its 1167 nucleotide sites being polymorphic. Despite coding region conservation at the population level, the many non-synonymous mutations that exist in the *OXTR* coding sequences we examined imply that structural alterations have taken place in all functional domains in the mature OXTR protein (Figs. 3 and 4, Table 4). In general, NWP primates exhibit many more synonymous and non-synonymous mutations in the coding sequence of *OXTR* than OWP and APES. Each of the seven NWP genera examined (*Aotus*, *Lagothrix*, *Saguinus*, *Callithrix*, *Callicebus*, *Pithecia* and *Saimiri*) exhibits a number of lineage-specific mutations that distinguishes their *OXTR* coding sequences from those of any other taxon we investigated. *Aotus* samples exhibit four lineage-specific amino acid substitutions (positions 141, 177, 351 and 357). Moreover, *Callithrix*, *Saimiri* and *Saguinus* possess nearly twice as many amino acid changes (from 39 sequence consensus) than do other NWP, and feature a faster rate of mutational accumulation according to the BEAST analysis (Fig. 7). Interestingly, these three genera also exhibit variation in their social systems, and do not share any specific amino acid changes. Furthermore, all primate *OXTR* coding sequences differ from those of the two rodent species, which lack codon 252 (alanine), suggesting that the presence/absence of this amino acid residue is either a shared derived deletion in rodents, or a shared derived insertion in primates.

Another point of interest is the pattern of amino acid substitution that is exhibited in interspecific comparisons of the ligand-binding domain (codon positions 1–39, 93–114, and

173–201 (Chini et al., 1997; Gimpl and Fahrenholz, 2001; Wesley et al., 2002). Lee et al. (2011) discovered that certain NWP primates (*Saimiri sciureus*, *Cebus apaella*, *Aotus nancymaae* and *Callithrix jacchus*) produce a unique form of the OT neuropeptide that contains a Proline at position 8, whereas the other NWP primate examined in that study, the coppery titi monkey (*Callicebus cupreus*), shared the Leucine residue that is observed in all other placental mammals. Given the relatively high binding specificity of the OT ligand with the extremely selective OXTR receptor protein, as demonstrated in primate brains (*Macaca mulatta* and *Callicebus cupreus*, Freeman et al., 2014a, 2014b), it would seem likely that commensurate changes in the ligand binding domain of *OXTR* would have arisen in *Saimiri*, *Cebus*, *Aotus* and *Callithrix* to maintain proper ligand–receptor activity for animals with the Leu8Pro substitution in the OT nonapeptide.

Recent research by Vargas-Pinilla et al. (2015) explored this question, and suggested that the Phenylalanine-to-Tyrosine substitution at *OXTR* ligand-binding residue 103 in *Saimiri sciureus* may have coevolved with the Leu8Pro OT substitution, as *OXTR* position 103 is a binding site for OT position 8. Our data would tend to support this view, as all *Aotus* individuals (with the exception of AL01) also exhibit a Phenylalanine to Tyrosine substitution at *OXTR* 103. However, not one of the *Callithrix* or *Saguinus* samples that we analyzed exhibits this substitution. In fact, we do not observe any non-synonymous substitutions that are exclusive to our *Saimiri*, *Aotus*, *Callithrix* and *Saguinus* samples relative to other NWP samples, which share a total of 9 changes that distinguish them from OWP and APES (positions 5, 33, 169, 172, 248, 249, 251, 349 and 388). While protein binding assays would be necessary to confirm the interaction of the unique NWP OT ligand form(s) to the different NWP *OXTR* receptor ligand-binding domains, these findings strongly suggest that the entire OT pathway has different functional properties in NWP than in other primate taxa, possibly influencing the manifestation of the different social and mating systems (e.g., monogamy, polyandry) observed among some NWP species. However, we would also argue that the coevolution of OT-OXTR binding is more complex than the relationship of two residues, and is potentially linked to the adaptive radiation of NWP, rather than strictly the forces of positive selection.

4.3. No specific form of OXTR discretely clusters with socially monogamous primate taxa

In our analysis of *OXTR* 5′ regulatory and coding sequence variation, we observed many distinct types of molecular differences that distinguish primate lineages from one another. Considerable nucleotide and codon diversity exists among closely related primate taxa (Fig. 3). In addition, the presence of large insertions, deletions and derived clusters of dinucleotide repeats in the *OXTR* 5′ regulatory region of *H. sapiens* and *P. troglodytes* add

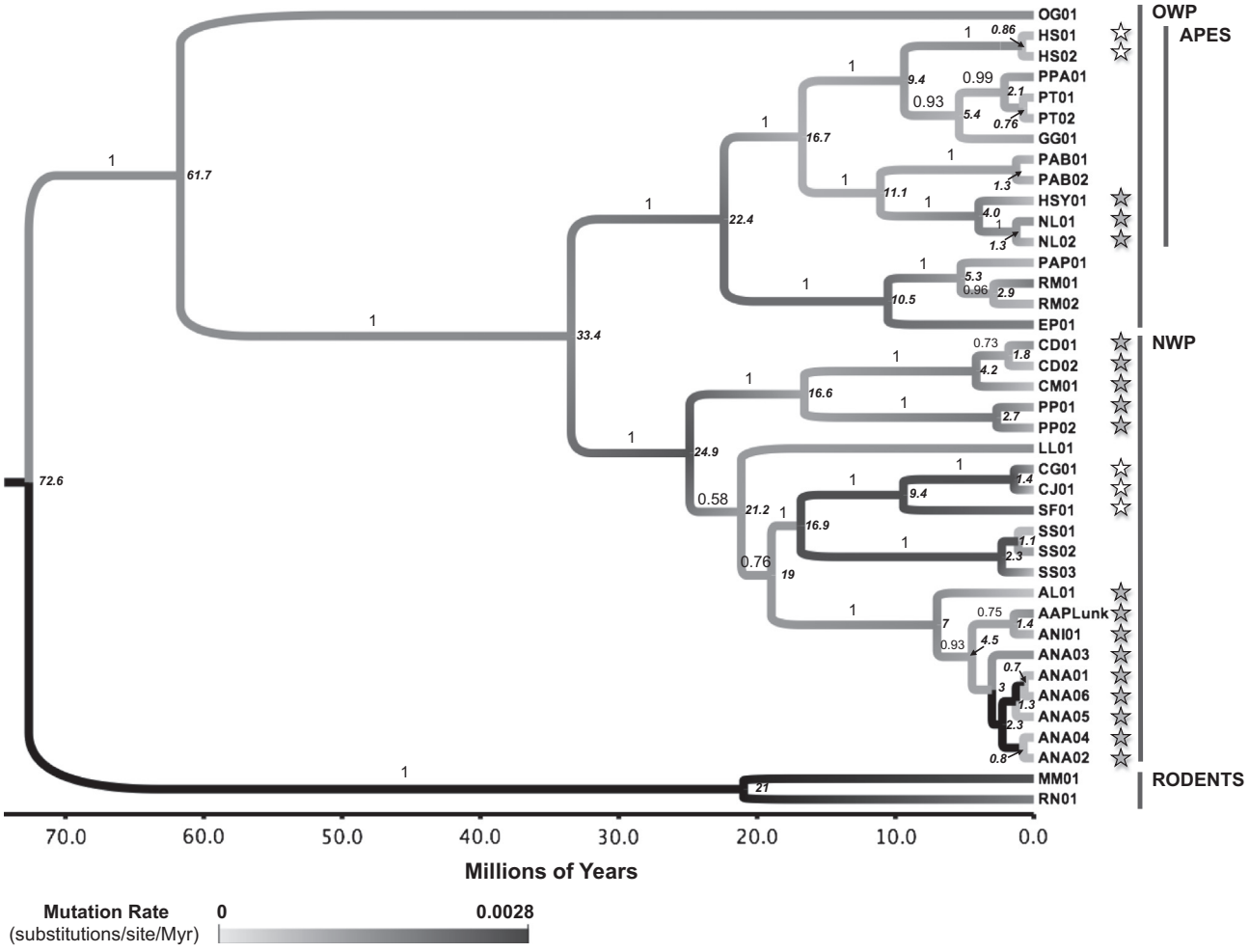

Fig. 7. A chronogram depicting the Bayesian coalescence age estimation of *OXTR* coding region sequences, as calculated in BEAST v1.5.4. Age estimates (in millions of years) for each node are italicized and positioned to the right of them. Posterior probabilities are indicated above each branch. The mutation rate of *OXTR* along the different evolutionary lineages is displayed as a gray scale gradient across taxa, with the key shown at the lower left. Broad phylogenetic clade memberships, drawn as *dark gray* vertical lines, are shown on the right.

another level of putatively functional variation. NWP share 9 derived amino acid substitutions in their *OXTR* coding sequences that separate their clade from other primates (Figs. 3 and 5). This pattern could have resulted from the adaptive radiation of the clade ~30 million years ago, or instead been a driver of (or a response to) the novel forms of the OT neuropeptide seen among some NWP taxa (Lee et al., 2011; Vargas-Pinilla et al., 2015). Furthermore, CNVs and STRs are present throughout the *OXTR* region in mammals, and can reportedly facilitate changes in gene expression in different species or individuals (Conrad et al., 2010; Gökçumen et al., 2011; Iskow et al., 2012). Together, these observations suggest that non-neutral variation, arising from both selective and demographic mechanisms, may be present at this locus across the Order Primates.

Despite the extensive and potential non-neutrality of the variation that exists at the *OXTR* locus in primates, no specific kind of molecular variation clusters with any particular social systems exhibited by primate taxa. This is especially clear in the case of monogamous social systems, which characterize the genera of *Aotus*, *Callicebus*, *Pithecia*, *Hylobates* (+*Nomascus*), and at least partially *Callithrix*, *Saguinus* and (arguably) *Homo*. Although five of these eight genera are NWP, none share obvious *OXTR* sequence characteristics with each other (whether considering regulatory or coding sequences) that distinguish them from their non-monogamous NWP relatives. Similarly, the sequences from monogamous APES, *Homo* and *Hylobates* (+*Nomascus*) are as similar to those of non-monogamous APE taxa *P. troglodytes*, *P. paniscus*, *P. pygmaeus abelii*, and *G. gorilla*, as they are to one another (pairwise identity, 99.2%). These data reinforce the hypothesis that monogamy has arisen multiple times in the primate order through different molecular mechanisms, and that 5′ regulatory and coding variation at the *OXTR* gene does not explain the phylogenetic patterning of monogamy in primates.

5. Conclusions

To summarize, despite the biological importance of maintaining a functional OT pathway, as evidenced by the high levels of intraspecific sequence conservation in Azara's owl monkeys and in humans, our findings suggest that the *OXTR* locus has undergone a considerable amount of evolutionary change among primate species. We observe substantial variation in the putative 5′ regulatory region of *OXTR*, with marked structural differences across primate taxa, particularly for humans (*H. sapiens*) and chimpanzees (*P. troglodytes*), which exhibit unique patterns of large motifs of dinucleotide A + T repeats upstream of the *OXTR* 5′ UTR. In addition, we observe a large number of amino acid substitutions in the *OXTR* CDS region among NWP taxa that distinguish them from their OWP relatives. Moreover, primate taxa traditionally defined as socially monogamous (e.g., gibbons, owl monkeys, titi monkeys, and saki monkeys) all exhibit different amino acid motifs for their respective *OXTR* protein coding sequences. These findings support the notion that monogamy has evolved independently in Old World and New World primates, and that it has done so through different molecular mechanisms, not exclusively through the oxytocin pathway.

Conflicts of interest

The authors declare no conflicting interests.

Acknowledgments

The authors would like to thank the many students, volunteers, and researchers who assisted with the capturing and sampling of the owl monkeys that led to the collection of samples used in the study. Special gratitude is owed to M. Rotundo for his assistance in the field during the past decade. We also thank Mr. John Adams, Mr. F. Middleton, Ing. C. Cimino and Ing. A. Casaretto for their continuing support at Estancia Guaycolec. The Ministerio de la Producción, Subsecretaría de Ecología and Recursos Naturales from Formosa Province, and the Dirección de Fauna Silvestre de la Nación Argentina authorized and supported the research. In addition, the authors would like to share their appreciation for the biological samples provided by O. Ryder at the San Diego Zoo, and S. Evans at the DuMond Conservancy, and thank J. Tinsman for assistance with sequencing work. This study was based upon work supported by the GAPSA-Provost Award for Interdisciplinary Innovation from the University of Pennsylvania (PLB), a General Research Grant from the L.S.B. Leakey Foundation (PLB), and research funds from the Department of Anthropology at the University of Pennsylvania (PLB). EFD also acknowledges financial support from the University Research Fund at the University of Pennsylvania, the Wenner-Gren Foundation, the L.S.B. Leakey Foundation, the National Geographic Society, the National Science Foundation (BCS-0621020) and the Zoological Society of San Diego. TGS further acknowledges the infrastructural support from the National Geographic Society. The authors would also like to thank two anonymous reviewers for their helpful comments on an earlier version of the manuscript.

Appendix A. Supplementary material

Supplementary data associated with this article can be found, in the online version, at http://dx.doi.org/10.1016/j.ympev.2015.05.006.

References

1000 Genomes Project Consortium, 2010. A map of human genome variation from population-scale sequencing. Nature 467 (7319), 1061–1073.
1000 Genomes Project Consortium, 2012. An integrated map of genetic variation from 1092 human genomes. Nature 491 (7422), 56–65.
Altekar, G., Dwarkadas, S., Huelsenbeck, J.P., Ronquist, F., 2004. Parallel metropolis-coupled Markov Chain Monte Carlo for Bayesian phylogenetic inference. Bioinformatics 20, 407–415.
Babb, P.L., Fernandez-Duque, E., Schurr, T.G., 2010. AVPR1A sequence variation in monogamous owl monkeys (*Aotus azarae*) and its implications for the evolution of platyrrhine social behavior. J. Mol. Evol. 71, 279–297.
Babb, P.L., Fernandez-Duque, E., Baiduc, C.A., Gagneux, P., Evans, S., Schurr, T.G., 2011a. MtDNA diversity in Azara's owl monkeys (*Aotus azarai azarai*) of the Argentinean Chaco. Am. J. Phys. Anthropol. 146, 209–224.
Babb, P.L., McIntosh, A.M., Fernandez-Duque, E., Di Fiore, A., Schurr, T.G., 2011b. An optimized genotyping strategy for assessing genetic identity and kinship in Azara's owl monkeys (*Aotus azarai*). Folia Primatol. 82, 107–117.
Babb, P.L., McIntosh, A.M., Fernandez-Duque, E., Schurr, T.G., 2013. Prolactin receptor gene diversity in Azara's owl monkeys (*Aotus azarai*) and humans (*Homo sapiens*) suggests a non-neutral evolutionary history among primates. Int. J. Primatol. 35, 129–155.
Bales, K.L., Mason, W.A., Catana, C., Cherry, S.R., Mendoza, S.P., 2007a. Neural correlates of pair-bonding in a monogamous primate. Brain Res. 1184, 245–253.
Bales, K.L., van Westerhuyzen, J.A., Lewis-Reese, A.D., Grotte, N.D., Lanter, J.A., Carter, C.S., 2007b. Oxytocin has dose-dependent developmental effects on pair-bonding and alloparental care in female prairie voles. Horm. Behav. 52, 274–279.
Bales, K.L., Plotsky, P.M., Young, L.J., Lim, M.M., Grotte, N., Ferrer, E., Carter, C.S., 2007c. Neonatal oxytocin manipulations have long-lasting, sexually dimorphic effects on vasopressin receptors. Neuroscience 144, 38–45.
Bandelt, H.J., Forster, P., Röhl, A., 1999. Median-joining networks for inferring intraspecific phylogenies. Mol. Evol. Biol. 16, 37–48.
Barraza, J.A., Zak, P.J., 2009. Empathy toward strangers triggers oxytocin release and subsequent generosity. Ann. N. Y. Acad. Sci. 1167, 182–189.
Brotherton, P.N.M., Komers, P.E., 2003. Mate guarding and the evolution of social monogamy in mammals. In: Reichard, U.H., Boesch, C. (Eds.), Monogamy: Mating Strategies and Partnerships in Birds, Humans and Other Mammals. University of Cambridge Press, Cambridge, pp. 42–58.
Carter, C.S., 1998. Neuroendocrine perspectives on social attachment and love. Psychoneuroendocrinology 23, 779–818.

Carter, C.S., Grippo, A.J., Pournajafi-Nazarloo, H., Ruscio, M.G., Porges, S.W., 2008. Oxytocin, vasopressin and sociality. Prog. Brain Res. 170, 331–336.
Cavanaugh, J., Mustoe, A.C., Taylor, J.H., French, J.A., 2014. Oxytocin facilitates fidelity in well-established marmoset pairs by reducing sociosexual behavior toward opposite-sex strangers. Psychoneuroendocrinology 49, 1–10.
Chen, F.S., Kumsta, R., von Dawans, B., Monakhov, M., Ebstein, R.P., Heinrichs, M., 2011. Common oxytocin receptor gene (OXTR) polymorphism and social support interact to reduce stress in humans. Proc. Natl. Acad. Sci. USA 108, 19937–19942.
Chini, B., Mouillac, B., Ala, Y., Balestre, M.N., Trumpp-Kallmeyer, S., Hoflack, J., Elands, J., Hibert, M., Manning, M., Jard, S., Barberis, C., 1997. Identification of a single residue responsible for agonist selectivity in the oxytocin–vasopressin receptors. Ann. N. Y. Acad. Sci. 812, 218–221.
Conrad, D., Pinto, D., Redon, R., Feuk, L., Gökçumen, Ö., Zhang, Y., Aerts, J., Andrews, T.D., Barnes, C., Campbell, P., Fitzgerald, T., Hu, M., Ihm, C.H., Kristiansson, K., MacArthur, D.G., MacDonald, J.R., Onyiah, I., Pang, A.W., Robson, S., Stirrups, K., Valsesia, A., Walter, K., Wei, J., Wellcome Trust Case Control Consortium, Tyler-Smith, C., Carter, N.P., Lee, C., Scherer, S.W., Hurles, M.E., 2010. Common copy number variation in the human genome: mechanism, selection and disease association. Nature 464, 704–712.
Damiano, C.R., Aloi, J., Dunlap, K., Burrus, C.J., Mosner, M.G., Kozink, R.V., McLaurin, R.E., Mullette-Gillman, O.A., Carter, R.M., Huettel, S.A., McClernon, F.J., Ashley-Koch, A., Dichter, G.S., 2014. Association between the oxytocin receptor (OXTR) gene and mesolimbic responses to rewards. Mol. Autism 5, 7.
Danecek, P., Auton, A., Abecasis, G., Albers, C.A., Banks, E., DePristo, M.A., Handsaker, R.E., Lunter, G., Marth, G.T., Sherry, S.T., McVean, G., Durbin, R., 1000 Genomes Project Analysis Group, 2011. The variant call format and VCFtools. Bioinformatics 27, 2156–2158.
Darriba, D., Taboada, G.L., Doallo, R., Posada, D., 2012. jModelTest 2: more models, new heuristics and parallel computing. Nat. Methods 9, 772.
Down, T.A., Hubbard, T.J., 2002. Computational detection and location of transcription start sites in mammalian genomic DNA. Genome Res. 12, 458–461.
Drummond, A.J., Rambaut, A., 2007. BEAST: Bayesian evolutionary analysis by sampling trees. BMC Evol. Biol. 7, 214.
Drummond, A.J., Nicholls, G.K., Rodrigo, A.G., Solomon, W., 2002. Estimating mutation parameters, population history and genealogy simultaneously from temporally spaced sequence data. Genetics 161, 1307–1320.
Drummond, A.J., Ho, S.Y.W., Phillips, M.J., Rambaut, A., 2006. Relaxed phylogenetics and dating with confidence. PLoS Biol. 4, e88.
Drummond, A.J., Ashton, B., Cheung, M., Heled, J., Kearse, M., Moir, R., Stones-Havas, S., Thierer, T., Wilson, A., 2010. Geneious 5.0. <http://www.geneious.com>.
Felsenstein, J., 2005. PHYLIP (Phylogeny Inference Package) v3.6. <http://evolution.genetics.washington.edu/phylip.html>.
Fernandez-Duque, E., 2009. Natal dispersal in monogamous owl monkeys (*Aotus azarai*) of the Argentinean Chaco. Behaviour 146, 583–606.
Fernandez-Duque, E., 2015. Social monogamy in wild owl monkeys (*Aotus azarae*) of Argentina: the potential influences of resource distribution and ranging patterns. Am. J. Primatol. (in press). http://dx.doi.org/10.1002/ajp.22397, <http://onlinelibrary.wiley.com/doi/10.1002/ajp.22397/full>.
Fernandez-Duque, E., Huck, M., 2013. Till death (or an intruder) do us part: intrasexual-competition in a monogamous primate. PLoS One 8, e53724.
Fernandez-Duque, E., Rotundo, M., Sloan, C., 2001. Density and population structure of owl monkeys (*Aotus azarai*) in the Argentinean Chaco. Am. J. Primatol. 53, 99–108.
Flicek, P., Amode, M.R., Barrell, D., Beal, K., Brent, S., Chen, Y., Clapham, P., Coates, G., Fairley, S., Fitzgerald, S., Gordon, L., Hendrix, M., Hourlier, T., Johnson, N., Kähäri, A., Keefe, D., Keenan, S., Kinsella, R., Kokocinski, F., Kulesha, E., Larsson, P., Longden, I., McLaren, W., Overduin, B., Pritchard, B., Riat, H.S., Rios, D., Ritchie, G.R., Ruffier, M., Schuster, M., Sobral, D., Spudich, G., Tang, Y.A., Trevanion, S., Vandrovcova, J., Vilella, A.J., White, S., Wilder, S.P., Zadissa, A., Zamora, J., Aken, B.L., Birney, E., Cunningham, F., Dunham, I., Durbin, R., Fernández-Suarez, X.M., Herrero, J., Hubbard, T.J., Parker, A., Proctor, G., Vogel, J., Searle, S.M., 2011. Ensembl 2011. Nucl. Acids Res. 39, 800–806.
Freeman, S.M., Inoue, K., Smith, A.L., Goodman, M.M., Young, L.J., 2014a. The neuroanatomical distribution of oxytocin receptor binding and mRNA in the male rhesus macaque (*Macaca mulatta*). Psychoneuroendocrinology 45, 128–141.
Freeman, S.M., Walum, H., Inoue, K., Smith, A.L., Goodman, M.M., Bales, K.L., Young, L.J., 2014b. Neuroanatomical distribution of oxytocin and vasopressin 1a receptors in the socially monogamous coppery titi monkey (*Callicebus cupreus*). Neuroscience 273, 12–23.
Fuentes, A., 1999. Re-evaluating primate monogamy. Am. Anthropol. 100, 890–907.
Gimpl, G., Fahrenholz, F., 2001. The oxytocin receptor system: structure, function, and regulation. Physiol. Rev. 81 (2), 629–683.
Gökçumen, O.∗, Babb, P.L.∗, Iskow, R.C., Zhu, Q., Shi, X., Mills, R.E., Ionita-Laza, I., Vallender, E.J., Clark, A., Johnson, W.E., Lee, C., 2011. Refinement of primate CNV hotspots identifies candidate genomic regions evolving under positive selection. Genome Biol. 12, 1–11.
Gregory, S.G., Connelly, J.J., Towers, A.J., Johnson, J., Biscocho, D., Markunas, C.A., Lintas, C., Abramson, R.K., Wright, H.H., Ellis, P., Langford, C.F., Worley, G., Delong, G.R., Murphy, S.K., Cuccaro, M.L., Persico, A., Pericak-Vance, M.A., 2009. Genomic and epigenetic evidence for oxytocin receptor deficiency in autism. BMC Med. 7, e1–e13.
Grippo, A.J., Wu, K.D., Hassan, I., 2008. Social isolation in prairie voles induces behaviors relevant to negative affect: toward the development of a rodent model focused on co-occurring depression and anxiety. Depress Anxiety 25, e17–e26.
Grippo, A.J., Trahanas, D.M., Zimmerman, R.R.N., Porges, S.W., Carter, C.S., 2009. Oxytocin protects against negative behavioral and autonomic consequences of long-term social isolation. Psychoneuroendocrinology 34, 1542–1553.
Guindon, S., Gascuel, O., 2003. A simple, fast and accurate method to estimate large phylogenies by maximum-likelihood. Syst. Biol. 52, 696–704.
Hasegawa, M., Kishino, H., Yano, T., 1985. Dating of the human-ape splitting by a molecular clock of mitochondrial DNA. J. Mol. Evol. 22, 160–174.
Ho, S.Y.W., Phillips, M.J., Cooper, A., Drummond, A.J., 2005. Time dependency of molecular rate estimates and systematic overestimation of recent divergence times. Mol. Biol. Evol. 22, 1561–1568.
Hodgson, J.A., Sterner, K.N., Matthews, L.J., Burrell, A.S., Jani, R.A., Raaum, R.L., Stewart, C.B., Disotell, T.R., 2009. Successive radiations, not stasis, in the South American primate fauna. Proc. Natl. Acad. Sci. USA 106, 5534–5539.
Huck, M.A., Fernandez-Duque, E., 2013. When dads help: male behavioral care during primate infant development. In: Clancy, K., Hinde, K., Rutherford, J. (Eds.), Building Babies: Primate Development in Proximate and Ultimate Perspective. Springer Publishing, New York, pp. 361–385.
Huck, M., Fernandez-Duque, E., Babb, P., Schurr, T.G., 2014. Correlates of genetic monogamy in socially monogamous mammals: insights from Azara's owl monkeys. Proc. R. Soc. B 281, e1–e9.
Huelsenbeck, J.P., Ronquist, F., 2001. MrBayes: Bayesian inference of phylogenetic trees. Bioinformatics 17, 754–755.
Huelsenbeck, J.P., Ronquist, F., Nielsen, R., Bollback, J.P., 2001. Bayesian inference of phylogeny and its impact on evolutionary biology. Science 294, 2310–2314.
Iafrate, A.J., Feuk, L., Rivera, M.N., Listewnik, M.L., Donahoe, P.K., Qi, Y., Scherer, S.W., Lee, C., 2004. Detection of large-scale variation in the human genome. Nat. Genet. 36, 949–951.
Inoue, T., Kimura, T., Azuma, C., Inazawa, J., Takemura, M., Kikuchi, T., Kubota, Y., Ogita, K., Saji, F., 1994. Structural organization of the human oxytocin receptor gene. J. Biol. Chem. 269, 32451–32456.
Isberg, V., Vroling, B., van der Kant, R., Li, K., Vriend, G., Gloriam, D., 2014. GPCRDB: an information system for G protein-coupled receptors. Nucl. Acids Res. 42, 422–425.
Iskow, R.C.∗, Gökçumen, O.∗, Abyzov, A., Malukiewicz, J., Zhu, Q., Sukumar, A.T., Pai, A.A., Mills, R.E., Habegger, L., Cusanovich, D.A., Rubel, M.A., Perry, G.H., Gerstein, M., Stone, A.C., Gilad, Y., Lee, C., 2012. Regulatory element copy number differences shape primate expression profiles. Proc. Natl. Acad. Sci. USA 109, 12656–12661.
Itsara, A., Cooper, G.M., Baker, C., Girirajan, S., Li, J., Absher, D., Krauss, R.M., Myers, R.M., Ridker, P.M., Chasman, D.I., Mefford, H., Ying, P., Nickerson, D.A., Eichler, E.E., 2009. Population analysis of large copy number variants and hotspots of human genetic disease. Am. J. Hum. Genet. 84, 148–161.
Jacob, S., Brune, C.W., Carter, C.S., Leventhal, B.L., Lord, C., Cook Jr., E.H., 2007. Association of the oxytocin receptor gene (OXTR) in Caucasian children and adolescents with autism. Neurosci. Lett. 417, 6–9.
Jakobsson, M., Scholz, S.W., Scheet, P., Gibbs, J.R., VanLiere, J.M., Fung, H.C., Szpiech, Z.A., Degnan, J.H., Wang, K., Guerreiro, R., Bras, J.M., Schymick, J.C., Hernandez, D.G., Traynor, B.J., Simon-Sanchez, J., Matarin, M., Britton, A., van de Leemput, J., Rafferty, I., Bucan, M., Cann, H.M., Hardy, J.A., Rosenberg, N.A., Singleton, A.B., 2008. Genotype, haplotype and copy-number variation in worldwide human populations. Nature 451, 998–1003.
Karolchik, D., Barber, G.P., Casper, J., Clawson, H., Cline, M.S., Diekhans, M., Dreszer, T.R., Fujita, P.A., Guruvadoo, L., Haeussler, M., Harte, R.A., Heitner, S., Hinrichs, A.S., Learned, K., Lee, B.T., Li, C.H., Raney, B.J., Rhead, B., Rosenbloom, K.R., Sloan, C.A., Speir, M.L., Zweig, A.S., Haussler, D., Kuhn, R.M., Kent, W.J., 2014. The UCSC Genome Browser database: 2014 update. Nucl. Acids Res. 42, 764–770.
Keinan, A., Clark, A., 2012. Recent explosive human population growth has resulted in an excess of rare genetic variants. Science 336, 740–743.
Kent, W.J., 2002. BLAT – the BLAST-like alignment tool. Genome Res. 12, 656–664.
Kent, W.J., Sugnet, C.W., Furey, T.S., Roskin, K.M., Pringle, T.H., Zahler, A.M., Haussler, D., 2002. The human genome browser at UCSC. Genome Res. 12, 996–1006.
Kim, J.I., Ju, Y.S., Park, H., Kim, S., Lee, S., Yi, J.H., Mudge, J., Miller, N.A., Hong, D., Bell, C.J., Kim, H.S., Chung, I.S., Lee, W.C., Lee, J.S., Seo, S.H., Yun, J.Y., Woo, H.N., Lee, H., Suh, D., Lee, S., Kim, H.J., Yavartanoo, M., Kwak, M., Zheng, Y., Lee, M.K., Park, H., Kim, J.Y., Gökçumen, O., Mills, R.E., Zaranek, A.W., Thakuria, J., Wu, X., Kim, R.W., Huntley, J.J., Luo, S., Schroth, G.P., Wu, T.D., Kim, H., Yang, K.S., Park, W.Y., Kim, H., Church, G.M., Lee, C., Kingsmore, S.F., Seo, J.S., 2009. A highly annotated whole-genome sequence of a Korean individual. Nature 460, 1011–1015.
Kimura, T., Tanizawa, O., Mori, K., Brownstein, M.J., Okayama, H., 1992. Structure and expression of a human oxytocin receptor. Nature 356, 526–529.
Lee, A.G., Cool, D.R., Grunwald, W.C., Neal, D.E., Buckmaster, C.L., Cheng, M.Y., Hyde, S.A., Lyons, D.M., Parker, K.J., 2011. A novel form of oxytocin in New World monkeys. Biol. Lett. 7, 584–587.
Lukas, D., Clutton-Brock, T.H., 2013. The evolution of social monogamy in mammals. Science 341, 526–530.
Mendoza, S.P., Reeder, D.M., Mason, W.A., 2002. Nature of proximate mechanisms underlying primate social systems: simplicity and redundancy. Evol. Anthropol. 11, 112–116.
Mitani, J., Call, J., Kappeler, P., Palombit, R., Silk, J., 2012. The Evolution of Primate Societies. University of Chicago Press, Chicago, 744pp.
Moller, A.P., 2003. The evolution of monogamy: mating relationships, parental care and sexual selection. In: Reichard, U.H., Boesch, C. (Eds.), Monogamy: Mating Strategies and Partnerships in Birds, Humans and Other Mammals. University of Cambridge Press, Cambridge, pp. 29–41.

Nei, M., Li, W.H., 1979. Mathematical model for studying genetic variation in terms of restriction endonucleases. Proc. Natl. Acad. Sci. USA 76, 5269–5273.
Opazo, J.C., Wildman, D.E., Prychitko, T., Johnson, R.M., Goodman, M., 2006. Phylogenetic relationships and divergence times among New World monkeys (Platyrrhini, Primates). Mol. Phylogenet. Evol. 40, 274–280.
Paradis, E., 2010. pegas: an R package for population genetics with an integrated-modular approach. Bioinformatics 26, 419–420.
Paradis, E., Claude, J., Strimmer, K., 2004. APE: analyses of phylogenetics and evolution in R language. Bioinformatics 20, 289–290.
Perelman, P., Johnson, W.E., Roos, C., Seuánez, H.N., Horvath, J.E., Moreira, M.A., Kessing, B., Pontius, J., Roelke, M., Rumpler, Y., Schneider, M.P., Silva, A., O'Brien, S.J., Pecon-Slattery, J., 2011. A molecular phylogeny of living primates. PLoS Genet. 7, e1001342.
Pinto, D., Marshall, C., Feuk, L., Scherer, S.W., 2007. Copy-number variation in control population cohorts. Hum. Mol. Genet. 16, 168–173.
Posada, D., 2008. jModelTest: phylogenetic model averaging. Mol. Biol. Evol. 25, 1253–1256.
Poux, C., Chevret, P., Huchon, D., De Jong, W.W., Douzery, E.J.P., 2006. Arrival and diversification of caviomorph rodents and platyrrhine primates in South America. Syst. Biol. 55, 228–244.
Prado-Martinez, J., Sudmant, P.H., Kidd, J.M., Li, H., Kelley, J.L., Lorente-Galdos, B., Veeramah, K.R., Woerner, A.E., O'Connor, T.D., Santpere, G., Cagan, A., Theunert, C., Casals, F., Laayouni, H., Munch, K., Hobolth, A., Halager, A.E., Malig, M., Hernandez-Rodriguez, J., Hernando-Herraez, I., Prüfer, K., Pybus, M., Johnstone, L., Lachmann, M., Alkan, C., Twigg, D., Petit, N., Baker, C., Hormozdiari, F., Fernandez-Callejo, M., Dabad, M., Wilson, M.L., Stevison, L., Camprubí, C., Carvalho, T., Ruiz-Herrera, A., Vives, L., Mele, M., Abello, T., Kondova, I., Bontrop, R.E., Pusey, A., Lankester, F., Kiyang, J.A., Bergl, R.A., Lonsdorf, E., Myers, S., Ventura, M., Gagneux, P., Comas, D., Siegismund, H., Blanc, J., Agueda-Calpena, L., Gut, M., Fulton, L., Tishkoff, S.A., Mullikin, J.C., Wilson, R.K., Gut, I.G., Gonder, M.K., Ryder, O.A., Hahn, B.H., Navarro, A., Akey, J.M., Bertranpetit, J., Reich, D., Mailund, T., Schierup, M.H., Hvilsom, C., Andrés, A.M., Wall, J.D., Bustamante, C.D., Hammer, M.F., Eichler, E.E., Marques-Bonet, T., 2013. Great ape genetic diversity and population history. Nature 499, 471–475.
R Core Team, 2012. R: A Language and Environment for Statistical Computing. R Foundation for Statistical Computing, Vienna, Austria. <http://www.R-project.org/>.
Rambaut, A., 2014. FigTree v1.4.2. <http://beast.bio.ed.ac.uk/FigTree>.
Rambaut, A., Drummond, A.J., 2007. Tracer v1.5. <http://beast.bio.ed.ac.uk/Tracer>.
Ronquist, F., Huelsenbeck, J.P., 2003. MrBayes 3, Bayesian phylogenetic inference under mixed models. Bioinformatics 19, 1572–1574.
Rotundo, M., Fernandez-Duque, E., Dixson, A., 2005. Infant development and parental care in free-ranging *Aotus azarai azarai* in Argentina. Int. J. Primatol. 26, 1459–1473.
Rozen, S., Skaletsky, H., 2000. Primer3 on the WWW for general users and for biologist programmers. In: Krawetz, S., Misener, S. (Eds.), Bioinformatics Methods and Protocols: Methods in Molecular Biology. Humana Press, Totowa, NJ, pp. 365–386.
Shaikh, T.H., Gai, X., Perin, J.C., Glessner, J.T., Xie, H., Murphy, K., O'Hara, R., Casalunovo, T., Conlin, L.K., D'Arcy, M., Frackelton, E.C., Geiger, E.A., Haldeman-Englert, C., Imielinski, M., Kim, C.E., Medne, L., Annaiah, K., Bradfield, J.P., Dabaghyan, E., Eckert, A., Onyiah, C.C., Ostapenko, S., Otieno, F.G., Santa, E., Shaner, J.L., Skraban, R., Smith, R.M., Elia, J., Goldmuntz, E., Spinner, N.B., Zackai, E.H., Chiavacci, R.M., Grundmeier, R., Rappaport, E.F., Grant, S.F., White, P.S., Hakonarson, H., 2009. Genome Res. 19, 1682–1690.
Skuse, D.H., Lori, A., Cubells, J.F., Lee, I., Conneely, K.N., Puura, K., Lehtimaki, T., Binder, E.B., Young, L.J., 2014. Common polymorphism in the oxytocin receptor gene (OXTR) is associated with human social recognition skills. Proc. Natl. Acad. Sci. USA 111, 1987–1992.
Smith, A.S., Agmo, A., Birnie, A.K., French, J.A., 2010. Manipulation of the oxytocin system alters social behavior and attraction in pair-bonding primates, *Callithrix penicillata*. Horm. Behav. 57, 255–262.
Snowdon, C.T., Pieper, B.A., Boe, C.Y., Cronin, K.A., Kurian, A.V., Ziegler, T.E., 2010. Variation in oxytocin is related to variation in affiliative behavior in monogamous, pairbonded tamarins. Horm. Behav. 58, 614–618.
Swofford, D.L., 2002. PAUP*: Phylogenetic Analysis using Parsimony (and Other Methods), v4.0b10 Beta. Sinauer Associates, Sunderland, MA.
Tajima, F., 1989a. Statistical method for testing the neutral mutation hypothesis by DNA polymorphism. Genetics 123, 585–595.
Tajima, F., 1989b. The effect of change in population size on DNA polymorphism. Genetics 123, 597–601.
Takayanagi, Y., Yoshida, M., Bielsky, I.F., Ross, H.E., Kawamata, M., Onaka, T., Yanagisawa, T., Kimura, T., Matzuk, M.M., Young, L.J., Nishimori, K., 2005. Pervasive social deficits, but normal parturition, in oxytocin receptor-deficient mice. Proc. Natl. Acad. Sci. USA 102, 16096–16101.
Tansey, K.E., Brookes, K.J., Hill, M.J., Cochrane, L.E., Gill, M., Skuse, D., Correia, C., Vicente, A., Kent, L., Gallagher, L., Anney, R.J., 2010. Oxytocin receptor (OXTR) does not play a major role in the aetiology of autism: genetic and molecular studies. Neurosci. Lett. 474, 163–167.
Tost, H., Kolachana, B., Hakimi, S., Lemaitre, H., Verchinski, B.A., Mattay, V.S., Weinberger, D.R., Meyer-Lindenberg, A., 2010. A common allele in the oxytocin receptor gene (OXTR) impacts prosocial temperament and human hypothalamic–limbic structure and function. Proc. Natl. Acad. Sci. USA 107, 13936–13941.
Vargas-Pinilla, P., Paixão-Côrtes, V.R., Paré, P., Tovo-Rodrigues, L., Vieira, C.M., Xavier, A., Comas, D., Pissinatti, A., Sinigaglia, M., Rigo, M.M., Vieira, G.F., Lucion, A.B., Salzano, F.M., Bortolini, M.C., 2015. Evolutionary pattern in the OXT-OXTR system in primates: coevolution and positive selection footprints. Proc. Natl. Acad. Sci. USA 112, 88–93.
Wartmann, F.M., Juárez, C.P., Fernandez-Duque, E., 2014. Size, site fidelity and overlap of home ranges and core areas in the socially monogamous owl monkey (*Aotus azarai*) of Northern Argentina. Int. J. Primatol. 35, 919–939.
Wesley, V.J., Hawtin, S.R., Howard, H.C., Wheatley, M., 2002. Agonist-specific, high-affinity binding epitopes are contributed by an arginine in the N-terminus of the human oxytocin receptor. Biochemistry 41, 5086–5092.
Wildman, D.E., Jameson, N.M., Opazon, J.C., Yi, S.V., 2009. A fully resolved genus level phylogeny of neotropical primates (Platyrrhini). Mol. Phylogenet. Evol. 53, 694–702.
Wittig, R.M., Crockford, C., Deschner, T., Langergraber, K.E., Ziegler, T.E., Zuberbühler, K., 2014. Food sharing is linked to urinary oxytocin levels and bonding in related and unrelated wild chimpanzees. Proc. R. Soc. B 281, 20133096.
Wolovich, C.K., Perea-Rodriguez, J.P., Fernandez-Duque, E., 2008. Food transfers to young and mates in wild owl monkeys (*Aotus azarai*). Am. J. Primatol. 70, 211–221.
Wu, S., Jia, M., Ruan, Y., Liu, J., Guo, Y., Shuang, M., Gong, X., Zhang, Y., Yang, X., Zhang, D., 2005. Positive association of the oxytocin receptor gene (OXTR) with autism in the Chinese Han population. Biol. Psychiatry 58, 74–77.
Wu, N., Li, Z., Su, Y., 2012. The association between oxytocin receptor gene polymorphism (OXTR) and trait empathy. J. Affect. Disord. 138, 468–472.
Yang, Z., 2007. PAML 4: a program package for phylogenetic analysis by maximum likelihood. Mol. Biol. Evol. 24, 1586–1591.